Agricultural Water Management 283 (2023) 108306

Contents lists available at ScienceDirect

Agricultural Water Management

journal homepage: www.elsevier.com/locate/agwat

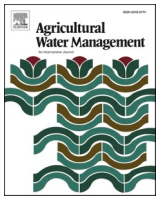

Salts dynamics in maize irrigation in the Hetao plateau using static water table lysimeters and HYDRUS-1D with focus on the autumn leaching irrigation

Tiago B. Ramos [a,*,1], Meihan Liu [b,c,1], Paula Paredes [d], Haibin Shi [c,**], Zhuangzhuang Feng [c], Huimin Lei [b], Luis S. Pereira [d]

[a] Centro de Ciência e Tecnologia do Ambiente e do Mar (MARETEC–LARSyS), Instituto Superior Técnico, Universidade de Lisboa, Av. Rovisco Pais, 1, 1049-001 Lisboa, Portugal
[b] State Key Laboratory of Hydroscience and Engineering, Department of Hydraulic Engineering, Tsinghua University, Beijing 100084, China
[c] College of Water Conservancy and Civil Engineering, Inner Mongolia Agricultural University, Hohhot 010018, China
[d] LEAF—Linking Landscape, Environment, Agriculture and Food Research Center, Associated Laboratory TERRA, Instituto Superior de Agronomia, Universidade de Lisboa, Tapada da Ajuda, 1349-017 Lisboa, Portugal

ARTICLE INFO

Handling Editor: Dr R Thompson

Keywords:
Autumn irrigation
Electrical conductivity of the soil saturation paste extract
Evapotranspiration
HYDRUS-1D model
Leaching
Upward fluxes

ABSTRACT

Soil salinization problems are widespread in the Hetao plain, Inner Mongolia, resulting from arid climate conditions, a shallow saline water table, poor irrigation water management, and insufficient drainage. This study follows previous research aimed at evaluating crop water use and controlling the salinity build-up in the region, namely using weighing and static water table lysimeters to parameterize a water balance model aimed at the development of appropriate irrigation scheduling. Two sets of five static water table lysimeters, which fixed depths ranged from 1.25 to 2.25 m, were used over two maize crop seasons. The mechanistic HYDRUS-1D model was further used to daily predict measured data on soil water contents, boundary fluxes in the interface between the saturated and unsaturated zones, the electrical conductivity of the soil saturation paste extract (EC_e), and the actual crop evapotranspiration ($ET_{c\ act}$). The soil water balance helped quantify the combined effect of water and salinity stresses on root water uptake as well as groundwater fluxes into the rootzone. The salt balance showed that the salinity build-up was much related to irrigation and capillary fluxes, and that the autumn irrigation carried out during the non-growing season was essential for controlling soil salinity. The efficiency of the autumn irrigation much depended on groundwater depth and the amount of water applied for salt leaching, with the best results found for the lysimeters with water table depths at 2.0 and 2.25 m (85–100%) for irrigation depths $\geq$ 220 mm. The lysimeters with shallower water tables never showed a leaching efficiency higher than 88%. This research shows that the sustainability of irrigation in Hetao depends on finding adequate solutions for controlling the depth of the saline groundwater, minimizing capillary fluxes to the rootzone, and developing consequent approaches for autumn irrigation leaching.

1. Introduction

Soil salinization is a major abiotic constraint in regions of arid to dry sub-humid climates. The best available estimates suggest that about 412 million ha are affected by salinity and 618 million ha by sodicity, either due to natural or human-induced processes (FAO, 2015). The human-induced causes, also referred to as secondary salinization, are mostly associated with the poor management of irrigation water, with factors such as climate conditions, soil properties, irrigation method, and associated soil and water management practices influencing the dynamics of salts in the soil profile and the degree to which crops are affected (Rhoades et al., 1992; Hoffman and Shalhevet, 2007; Pereira et al., 2014; Hopmans et al., 2021). Improving the sustainable management of irrigation water under saline conditions is thus critical to

* Correspondence to: MARETEC–LARSyS, Instituto Superior Técnico, Av. Rovisco Pais, 1049-001 Lisbon, Portugal.
** Corresponding author.
E-mail addresses: tiagobramos@tecnico.ulisboa.pt, tiago_ramos@netcabo.pt (T.B. Ramos), shi_haibin@aliyun.com (H. Shi).
[1] Equal contribution to this work.

https://doi.org/10.1016/j.agwat.2023.108306
Received 26 February 2023; Received in revised form 31 March 2023; Accepted 3 April 2023
Available online 10 April 2023

cope with the increasing water scarcity of salt-affected regions. Finding innovative water management techniques and strategies is required to improve crop water use while controlling the salt balance in the soil-water system, preventing salt accumulation in the root zone, and minimizing the damaging effect of salinity on crop transpiration and yield (Minhas et al., 2020).

The Hetao plain, in Inner Mongolia, with an irrigated area of 570,000 ha, is an example of a region where secondary salinization has been contributing to the degradation of local soil and water resources (Xu et al., 2010, 2011; Liu et al., 2022a; Wu et al., 2023). Surface irrigation is a well-adapted irrigation method for the region because diverted water from the Yellow River has an extremely high concentration of sediments, which is detrimental to sprinkler and drip equipment. However, as typical of its traditional management, the long-term excessive water diversion associated with hydro-geological conditions, poor irrigation water management, and insufficient drainage, has led to the rise of the saline water table and widespread salinization of the soil root zone (Xu et al., 2010, 2011). Water saving measures that have been progressively implemented throughout the years include the optimization of irrigation scheduling and practices (Pereira et al., 2003, 2007; Miao et al., 2016; Bai et al., 2017), the precise land leveling of basins and ridge furrows (Bai et al., 2010; Miao et al., 2015, 2018; Dong et al., 2018), and the use of straw and plastic film mulching (Zhao et al., 2016; Qi et al., 2018; Dong et al., 2018). While some of those water saving techniques can also contribute to minimizing soil salinization risks in the rootzone, the main approach for salt leaching continues to be the surface basin or border irrigation practiced in autumn after crops harvesting and before soil water freezes, with large water depths applied (200 mm or more) to leach the full root zone. However, the effectiveness of such a technique may be constrained by the presence of shallow and saline water tables (Minhas et al., 2020) as salts can easily migrate back up due to poor soil drainage conditions, and to the gradients that may develop before or after the soil freezes as the topsoil layers dry up. Furthermore, the autumn irrigation may not be compatible with the characteristics of modern irrigation systems such as drip, which are becoming increasingly used in Hetao, further stressing the importance of finding new approaches to control soil salinity.

The current study aims at evaluating the effectiveness of autumn irrigation for salinity control in Hetao and follows the companion papers dealing with crop water use under saline conditions in the region (Liu et al., 2022a, 2022b). Both studies evaluated the crop water use and the soil water balance of maize under saline conditions using weighing and static water table lysimeters, respectively, over three growing seasons. In both studies, the SIMDualKc model was used to successfully simulate the partition of crop evapotranspiration into its components, soil evaporation and crop evaporation, following the FAO56 dual crop coefficient approach (Allen et al., 1998, 2005). The model was also able to quantify the groundwater contribution to crop evapotranspiration, the effect of the different stressors (water and salinity) on crop water use, and the water productivity of maize while accounting for the leaching needs. Because of its semi-empirical nature, the model could not simulate the salinity build-up in the soil profile, particularly in the presence of shallow saline water tables, nor assess the effectiveness of autumn irrigation for salinity control. For such evaluations, mechanistic water flux models are needed.

As reviewed by Liu et al. (2022a, 2022b), diverse mechanistic models have been adopted and adapted for simulating the soil water dynamics and solute transport under Hetao's shallow saline groundwater conditions (e.g., Xu et al., 2015; Ren et al., 2016; Xue and Ren, 2017; Xiong et al., 2021). Most models were subjected to extensive calibration/validation for simulating the salinity build-up in the soil profile and impacts on crop growth and yields, but the effectiveness of salinity control measures, ancient or new, have rarely been assessed. Nevertheless, various studies focusing on the Hetao plateau have recognized the importance of the autumn irrigation for controlling salinity and improving soil conditions for plant germination and growth, e.g., Xu et al., (2010, 2011), Miao et al. (2015), and Liu et al. (2022a, 2022b). However, rare are studies attempting to identify the best application depths and relate them to the WTD (Liu et al., 2022c). Meanwhile, modelling applications have further been used for finding a suitable groundwater depth for crop growth (Pereira et al., 2007; Ma et al., 2008; Xu et al., 2013), lacking yet appropriate validation using data such as those obtained from the referred lysimeter studies.

As such, the specific objectives of this study are: (i) to calibrate/validate the HYDRUS-1D model (Šimůnek et al., 2016) for simulating soil water contents, boundary fluxes in the interface between the saturated and unsaturated zones, the electrical conductivity of the saturation paste extract (EC_e), and the actual crop evapotranspiration ($ET_{c\ act}$) using the static water table lysimeters data from the companion paper by Liu et al. (2022b); (ii) to compute the soil water and salt balances in the various lysimeters over the 2017 and 2018 maize growing seasons; and (iii) to evaluate the effectiveness of autumn irrigation for salt leaching when different application depths are used. The results of this study can contribute to the development of new approaches for salt control in the Hetao region, and the sustainable use of soil and water resources.

2. Material and methods

2.1. Study region and experimental data

This study is part of the investigation covered in companion paper Liu et al. (2022b), which presents the experimental data obtained in two sets of five static water-table lysimeters placed at the Shuguang Experimental Station, Hetao plain, Inner Mongolia, China (40°46′N, 107°24′E, 1039.6 m a.s.l.) during three maize growing seasons (2017–2019). As such, only information relevant to the current modeling study, which used data collected in 2017 and 2018, will be given here. The 2019 data were not considered as management conditions drastically changed in that season when no irrigation occurred.

The climate in the Hetao plain is arid continental. The mean annual precipitation is 137 mm (40 years average), mostly occurring in summer. The annual temperature ranges from - 10 °C in January to 25 °C in July, and the number of frost-free days ranges from 135 to 150. The weather data for the study period was obtained from a nearby automatic weather station placed over a well-watered clipped grass and included the maximum and minimum air temperatures (T_{max}, T_{min}, °C), the mean and minimum relative humidity (RH_{mean}, RH_{min}, %), the number of sunshine hours (n_{sun}, h), and the wind speed measured at 2 m height (u_2, m s^{-1}). These data were used to compute the daily reference evapotranspiration (ET_o, mm) with the FAO-56 Penman-Monteith (PM) equation (Allen et al., 1998). Daily precipitation (P, mm) was also obtained at the same weather station, so completing the daily weather data. Fig. 1 shows the information of interest to this study, i.e., the daily values of ET_o and precipitation during the study period.

The soil is silty loam, with the main physical properties presented in Table 1 while the methodology used for soil sampling and their determination is detailed in the companion paper by Liu et al. (2022a). The groundwater table is saline, with the electrical conductivity (EC_{gw}) averaging 1.85 and 1.75 dS m^{-1} in 2017 and 2018, respectively (Liu et al., 2022b).

Lysimeters were 3.3 m long × 2.0 m wide × 2.6 m deep, placed within a maize field (8.6 ha), and distanced not less than 100 m from the field edges to guarantee that the boundary layer of air above lysimeters was in equilibrium (Allen et al., 1991a,1991b; Allen et al., 2011a,2011b; Wright, 1991). Mariotte bottles were used to supply a stable water flow rate at the lysimeters bottom to maintain the targeted groundwater depth. The consumed water was measured every day at 8:00 am, with volume differences in the Mariotte bottles between two consecutive days corresponding to the portion of the groundwater used by the plants. The Mariotte bottles were then refilled back to the initial mark using groundwater pumped from a nearby well. In addition, drainage bottles were used to collect and measure the excess applied water relative to the

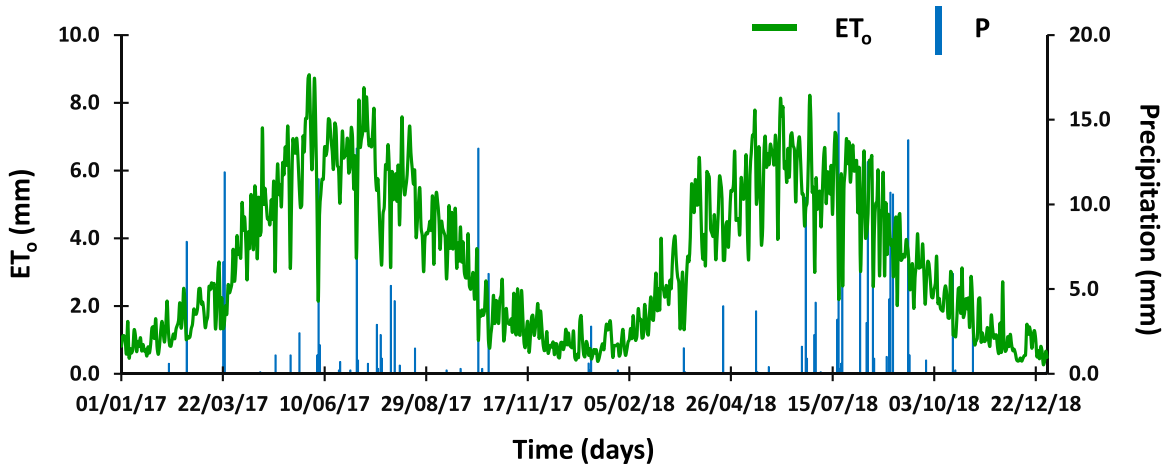

Fig. 1. Daily values of the reference evapotranspiration (ET_o) and precipitation (P) during the 2017 and 2018 seasons.

Table 1
Main physical and hydraulic properties of the soil in lysimeters.

Depth (m)	Particle size distribution (%)			ρ_b (g cm^{-3})	OM (%)	θ_{sat} (cm^3 cm^{-3})	θ_{FC} (cm^3 cm^{-3})	θ_{WP} (cm^3 cm^{-3})
	Clay (<0.002 mm)	Silt (0.002–0.05 mm)	Sand (>0.05 mm)					
0.0–0.1	3.3	64.4	32.3	1.45	0.81	0.43	0.34	0.13
0.1–0.2	3.2	72.4	24.4	1.44	0.69	0.44	0.34	0.13
0.2–0.4	2.9	77.8	19.2	1.46	0.97	0.45	0.35	0.14
0.4–0.6	3.3	76.1	20.6	1.46	0.92	0.48	0.35	0.14
0.6–0.8	2.6	79.4	18.1	1.46	0.65	0.46	0.35	0.13
0.8–1.0	2.9	75.6	21.5	1.47	0.55	0.47	0.34	0.13
1.0–1.2	3.6	65.4	31.0	1.47	0.54	0.45	0.35	0.13
1.2–1.4	2.6	68.4	29.0	1.54	0.72	0.43	0.35	0.13
1.4–1.6	2.3	74.9	22.8	1.55	0.64	0.42	0.34	0.14

ρ_b, soil bulk density; OM; soil organic matter content; θ_{sat}, θ_{FC}, θ_{WP}, soil water content respectively at saturation, field capacity, and wilting point.

Table 2
Observed dates of the crop growth stages during the 2017 and 2018 seasons.

Year	Crop growth stages			
	Initial	Crop development	Mid-season	Late-season
2017	12/05–10/06	10/06–22/07	23/07–30/08	31/08–28/09
2018	28/04–30/05	30/05–07/07	08/07–31/08	01/09–25/09

fixed WTD. Lysimeters were placed under an automatic rain shelter to avoid rainfall influence and more precisely measure the upward fluxes from the different water table depths (WTD) and related impacts. Further details about the characteristics of the lysimeters are given by Liu et al. (2022b). The static lysimeters used in this study had the water table fixed at depths of 1.25, 1.5, 2.0, 2.25 m during both seasons, covering the range of WTD observed in the region (Xiong et al., 2021).

Maize (Xi-meng 3358) was sown inside and outside lysimeters to ensure a similitude of environmental conditions and the one-dimensionality of measurements (Allen et al., 1991a, 1991b). The sowing dates and the dates of the crop stages for each growing season are given in Table 2. Plants were distanced 0.3 m along the row, and 0.40 m between rows (83,333 plants ha^{-1}). A 0.2 mm thick transparent polyethylene film mulch was placed along plant rows, covering 75% of the lysimeters surface (4.95 m^2), to reduce soil evaporation and increase soil temperature. The remaining soil surface was left bare for the application of irrigation water, fertilizers, and herbicides, which management followed local recommended practices.

Four irrigation events were performed in each maize season (Table 3), which were defined based on the surface irrigation management practices usually carried out by local farmers. Irrigation water was pumped from the groundwater, conveyed by a PVC pipe, applied in the lysimeters bare surface, and monitored with water-meters. Lysimeters were also irrigated in autumn (200 mm) mainly to leach salts away from the rootzone. Lysimeters were further subjected to pre-sowing irrigation aiming at having adequate soil moisture for ensuring adequate plant emergence and development. Because model simulations were performed from the sowing date onwards, the pre-sowing irrigation was only accounted for when defining the initial soil moisture conditions and therefore not included in Table 3. The soil water contents (SWC) were measured every hour with FDR soil moisture sensors (WiTu Agricultural Technology, Shenyang, China). Calibration procedures for the FDR sensors are described in Liu et al. (2022b). The FDR sensors were placed

Table 3
Irrigation scheduling during the 2017 and 2018.

Irrigation seasons		Growing season irrigations (mm)				Autumn irrigation (mm)	Total irrigation (mm)
2017	Dates	21/06	12/07	04/08	29/08	01/11	
	Depths	90	82	82	82	200	536
2018	Dates	26/06	16/07	09/08	28/08	01/11	
	Depths	100	72	82	82	200	536

in all lysimeters at the depths of 0.1, 0.2, 0.4 m, and then at every 0.2 m down to the targeted WTD.

For the determination of the electrical conductivity, disturbed soil samples (0.1 kg) were collected inside the lysimeters at the same depths as the SWC measurements using a soil auger. The electrical conductivity of the 1:5 soil water extract ($EC_{1:5}$, dS m^{-1}) was then measured using a DDS-11A conductivity-meter (INESA Scientific Instrument, Shanghai, China) and converted to the electrical conductivity of the soil saturation paste extract (EC_e) as described in Liu et al. (2022b). Measurements were carried out approximately every 10 days during both seasons.

2.2. Modeling approach

2.2.1. Model description

The HYDRUS-1D software package (Šimůnek et al., 2016) was used to numerically simulate one-dimensional water flow and solute transport in variably-saturated porous media by solving the Richards and the Fickian-based convection–dispersion equations, respectively, as follows:

$$\frac{\partial \theta}{\partial t} = \frac{\partial}{\partial z}\left[K(h)\left(\frac{\partial h}{\partial z} + 1\right)\right] - S(h, z, t) \quad (1)$$

$$\frac{\partial \theta c}{\partial t} + \rho\frac{\partial \overline{c}}{\partial t} = \frac{\partial}{\partial z}\left(\theta D\frac{\partial c}{\partial z}\right) - \frac{\partial qc}{\partial z} \quad (2)$$

where θ is the volumetric soil water content ($L^3\ L^{-3}$), t is time (T), z is the vertical space coordinate (L), h is the soil pressure head (L), K is the hydraulic conductivity (LT^{-1}), S is the sink term accounting for water uptake by plant roots ($L^3\ L^{-3}\ T^{-1}$), c and $\overline{c}$ are solute concentrations in the liquid (M L^{-3}) and solid (M M^{-1}) phases, respectively, ρ is the soil bulk density (M L^{-3}), q is the volumetric flux density (L T^{-1}), and D is the hydrodynamic dispersion coefficient ($L^2\ T^{-1}$). Root growth was simulated using the Verhulst-Pearl logistic growth function (Hoffman and van Genuchten, 1983).

The flow equation considered the unsaturated soil hydraulic properties as described by the van Genuchten–Mualem functional relationships (Mualem, 1976; van Genuchten, 1980):

$$S_e(h) = \frac{\theta(h) - \theta_r}{\theta_s - \theta_r} = \frac{1}{(1 + |\alpha h|^{\eta})^{m}} \quad (3)$$

$$K(h) = K_s S_e^{\ell}\left[1 - \left(1 - S_e^{1/m}\right)^{m}\right]^2 \quad (4)$$

where S_e is the effective saturation (-), θ_r and θ_s are the residual and saturated water contents ($L^3\ L^{-3}$), respectively, K_s is the saturated hydraulic conductivity (L T^{-1}), α (L^{-1}) and η (-) are empirical shape parameters, ℓ is a pore connectivity/tortuosity parameter (-), and m= 1–1/η.

The sink term in the flow equation considered the macroscopic approach proposed by Feddes et al. (1978), where the potential root water uptake rate, i.e., the potential crop transpiration rate (T_c, L T^{-1}), is distributed over the root zone and reduced due to the presence of depth-varying water and salinity stressors to obtain the actual root water uptake rate or actual transpiration rate ($T_{c\ act}$, L T^{-1}). The Feddes et al. (1978) model was selected to describe the water stress response function. In this model, root water uptake is at the potential rate when h is between h_2 and h_3, drops off linearly when $h > h_2$ or $h < h_3$, and becomes zero when $h < h_4$ or $h > h_1$ (subscripts 1–4 denote different threshold pressure heads). For the effect of the salinity stress on root water uptake, the Maas (1990) salinity threshold and slope function was used. In this function, root water uptake is maximum when the EC_e is below the crop tolerance salinity threshold ($EC_{e\ threshold}$, dS m^{-1}), decreasing then linearly for a unit increase in salinity beyond the threshold (s, % per dS m^{-1}). Because HYDRUS-1D simulates the electrical conductivity of the soil solution (EC_{sw}), the relation EC_{sw}/EC_e ratio = 2 is assumed for conversion purposes following a common approximation used for soil water contents near field capacity in medium-textured soils (U.S. Salinity Laboratory Staff, 1954; Skaggs et al., 2006; Ramos et al., 2011). The effects of the water and salinity stresses were assumed to be multiplicative (van Genuchten, 1987).

The compensated root water uptake mechanism introduced by Šimůnek and Hopmans (2009) was further considered when computing root water uptake. This mechanism considers the capacity of maize to compensate for reduced root water uptake in water-stressed parts of the root zone by increasing uptake in other soil regions that are less stressed. A critical value of the water stress index (ω_c), also referred to as root adaptability factor (Jarvis, 1989), is defined, with values ranging from 0 to 1. The closer the values are to 1, the less the ability to compensate rootzone stresses.

The solute transport equation considered the electrical conductivity of the irrigation water (EC_{iw}) and the soil solution (EC_{sw}) as nonreactive tracers, meaning that no adsorption in the solid phase was possible (Ramos et al., 2011). No solute uptake by plants was considered.

2.2.2. Model setup

In each lysimeter, the soil domain was defined as a one-dimensional column with 2.6 m depth discretized using 261 nodes. The soil profile was relatively homogeneous as is characteristic of loess soils (Table 1). However, during model calibration, there was a need to distinguish the topsoil layer from the rest of the soil profile. Lysimeters included a 0.25 m thick filter layer with sand and gravel placed at the bottom. Therefore, the soil column was divided into 3 distinct layers, with depths of 0.0–0.4 m, 0.4–2.35 m, and 2.35–2.6 m. The soil hydraulic parameters were first defined for each soil layer according to the average values proposed by Carsel and Parrish (1988) for each soil texture class. Soil dispersivity (λ; cm) values were set according to Xu et al. (2015). The soil hydraulic and solute transport parameters of the top two layers were then subjected to calibration. The initial soil water contents were defined based on the calibrated measured data from the FDR soil moisture sensors. The initial EC_{sw} was also defined based on the measurements.

The upper boundary conditions were determined by the potential crop transpiration (T_c; mm) and soil evaporation (E_s; mm) rates, irrigation and rainfall fluxes, and the EC_{iw}. T_c and E_s values were computed daily following the dual crop coefficient (dual-K_c) approach (Allen et al., 1998, 2005) using the SIMDualKc model (Rosa et al., 2012) as documented in Liu et al. (2022b). T_c reductions due to water stress were computed with the defined parameters in Wesseling et al. (1991) for maize: $h_1 = -15$ cm, $h_2 = -30$ cm, $h_3 = -325$ to -600 cm, and $h_4 = -8000$ cm. T_c reductions due to salinity stress considered a $EC_{e\ threshold}$ value of 1.7 dS m^{-1}, and a s rate value of 12% per dS m^{-1} (Minhas et al., 2020). The conversion of these values into EC_{sw} as required by HYDRUS-1D assumed the $EC_{sw}/EC_e = 2$ ratio.

In all lysimeters, the maximum root depth was set at 1.0 m. Because this could not be directly observed in the lysimeters without causing a major disturbance, several model runs were made to find the most adequate root depth for each lysimeter. The best results were found in all lysimeters for the same depth. While some relationship between root depth and groundwater depth could be expected, irrigation and the fact that root water uptake does not necessarily increase with root length as axial conductance becomes limiting (Landsberg and Fowkes, 1978) justifies this option. Root water uptake was thus assumed to occur mostly in the topsoil layers. The lower boundary conditions were described through variable pressure head conditions, which were set according to the depth of the water table in each lysimeter.

2.2.3. Model calibration and validation

The HYDRUS-1D model was calibrated for each lysimeter using the 2018 dataset. It was never possible to find a unique set of parameters capable of reproducing field measurements in all lysimeters, mostly due to small differences related to soil hydraulic parameters. The option was thus to allow varying soil hydraulic data between lysimeters while

maintaining constant crop related parameters. Validation was then performed using the calibrated parameters in each lysimeter and the independent data set of 2017.

Calibration procedures followed a four-step approach and were initiated by minimizing the deviation between measured and simulated soil moisture data at different depths. In this first step, the soil hydraulic parameters θ_s, α, η, and K_s were obtained through inverse modeling of daily soil water content data following Šimunek and van Genuchten (1996). The weighting coefficients used for the different soil water content data points in the objective function to be minimized were all assumed to be 1 since the observation errors of the measurements were unknown (Ramos et al., 2006; González et al., 2015). The θ_r was not modified as this parameter usually has little influence on simulated time series of soil water contents and soil pressure heads (González et al., 2015; Jacques et al., 2002; Šimůnek et al., 1998). The connectivity/tortuosity $\curlywedge$ parameter was set to 0.5 following Mualem (1976). At the end of this first step, measured soil moisture data were generally well reproduced at different depths. However, the upward fluxes measured at the depths of the static water tables were not. Therefore, in a second step, the K_s values were manually adjusted following a trial-and-error procedure until deviations between model simulations and field measurements of the upward fluxes were well simulated. The parameters of the root growth function (root depth at time t) were also tunned. The third step of the calibration procedure focused on adjusting the soil dispersivity (λ) values of the different soil layers, also following a trial-and-error procedure until deviations between model simulations and field measurements of the EC_e values were minimized. In the fourth and final step, the ω_c was modified to minimize the deviations between model simulations and field measurements of actual evapotranspiration ($ET_{c\ act}$) data.

The statistical indicators used to evaluate the goodness-of-fit between observed and predicted soil moisture, upward fluxes in the interface between the vadose zone and groundwater, EC_e, and $ET_{c\ act}$ data were those recommended by Pereira et al. (2015): the regression coefficient of the linear regression through the origin (b_0); the coefficient of determination (R^2) of the ordinary least-squares regression between observed and predicted values; the root mean square error (RMSE); the ratio between the RMSE and the mean of the observed data (NRMSE); the percent bias of estimation (PBIAS); and the Nash and Sutcliffe (1970) modeling efficiency (NSE). The full description of the statistical indicators can be found in Moriasi et al. (2007) and Legates and McCabe (1999). In general, b_0 equal to 1 indicates that the predicted values are statistically identical to field measurements. R^2 values close to 1 show that the model can explain the variance of the observations. RMSE and NRMSE values close to zero indicate that estimation errors are small and model predictions are good. PBIAS values close to zero describe accurate model simulations, while negative or positive values indicate over- or under-estimation bias, respectively. NSE values close to 1 mean that model predictions are good as the residuals' variance is much smaller than the observed data variance. Contrarily, if NSE < 0, the observed mean is a better indicator than model predictions.

2.2.4. The salt balance and leaching efficiency

The salt balance (SB; kg ha^{-1}) was computed by considering the depth and salinity of irrigation water diverted into the soil, the depth and salinity of rainfall infiltrating the soil, and the depth and salinity of drainage water discharged from the soil, as follows (Wilcox and Resch, 1963; Bresler et al., 1982):

$$SB = (TSC_{iw} + TSC_{rain}) - TSC_{dw} = 0.64[(D_{iw}EC_{iw} + D_{rain}EC_{rain}) - D_{dw}EC_{dw}]10 \quad (5)$$

where TSC_{iw}, TSC_{rain}, and TSC_{dw} are the total salt content of irrigation water, rainfall, and drainage water (kg ha^{-1}), respectively; D_{iw}, D_{rain}, and D_{dw} are the depth of irrigation water, rainfall, and drainage water (mm), respectively; and EC_{iw}, EC_{rain}, and EC_{dw} are the electrical conductivity of irrigation water, rainfall, and drainage water (dS m^{-1}), respectively. The EC_{rain} was 0.10 dS m^{-1}, which is slightly below the value of 0.12 dS m^{-1} used by Phogat et al. (2018). Positive SB values refer to salt accumulation in the root zone layer while negative SB values refer to leaching from the same layer. The SB was computed daily, and results accumulated for the entire growing season (Table 3). The SB was further extended to the end of each year (December) so that the leaching resulting from autumn irrigation could be accounted for. The leaching efficiency (LE) was lastly determined in each lysimeter from the ratio of the collected drained salt mass to the applied salt mass (Grismer, 1990; Yang et al., 2019), as follows:

$$LE = \frac{TSC_{dw}}{TSC_{iw} + TSC_{rain}} \quad (6)$$

3. Results and discussion

3.1. Model parameterization

Table 4 presents the calibrated soil hydraulic and solute transport parameters of the various lysimeters. Differences between lysimeters were due to the natural variability of soil hydraulic properties, to which the accurate representation of soil water content and upward fluxes data was sensitive. For the topsoil layer (0.0–0.4 m), those differences were noticed on the shape parameters α and η of the soil water retention, $\theta(h)$, and soil hydraulic conductivity, K(h), curves. For the subsoil layer (0.4–2.35 m), differences between lysimeters were likewise found on the same shape parameters, as well as on the K_s. The variability of both soil hydraulic functions was relatively minor (Fig. 2), but still capable of impacting the soil water balance in the lysimeters.

The calibrated soil dispersivity values were set the same in all lysimeters (Table 4). For the topsoil layer (0.0–0–4 m) and especially for the subsoil (0.4–2.35 m) layer, the calibrated values were found to be higher than those reported in similar modeling applications performed in the Hetao region or nearby. Xu et al. (2013) set λ to 19 cm in soil layers with varying thicknesses from 0.3 to 0.5 m in a 3.0 m soil profile. Xu et al. (2015) set λ to 20 cm in 0.6–0.9 m thickness layers in a 1.5 m soil column. Ren et al. (2016, 2017) set λ to a range of values from 15 to 20 cm in soil layers with thickness from 0.4 to 1.6 m in a 3.0 m soil profile. Soil dispersivity values are scaled with travel distance (Vanderborght and Vereecken, 2007), which justifies the larger calibrated values in this study, namely for the subsoil layer which thickness was larger (1.95 m) than any considered in the applications cited above.

Lastly, ω_c was set to 0.9 in all lysimeters, which agrees with Šimůnek and Hopmans (2009) hypothesis that agricultural plants may have a relatively high ω_c and thus a limited ability to compensate for natural stresses. The value is higher than the 0.8 adopted by González et al. (2015) for maize under full and deficit irrigation in Brazil, but that study didn't hold data on measured $ET_{c\ act}$ for a better definition of that parameter.

3.2. Model performance

3.2.1. Soil water contents

Fig. 3 shows, as an example, the measured soil water contents in different soil layers and the respective HYDRUS-1D simulated values in the lysimeter with WTD= 1.25 m along both growing seasons. Higher variations of soil water contents were observed closer to the soil surface, which was associated with irrigation events, infiltration, redistribution, and root water uptake. At deeper depths, soil water contents were relatively stable and progressively closer to soil saturation with depth due to the proximity of the water table. The same dynamics were observed for the remaining lysimeters.

Table 5 presents the values of the statistical indicators used to evaluate the goodness-of-fit between measured and simulated soil water contents in all lysimeters. For 2018 (the calibration year), the regression

Table 4
Calibrated soil hydraulic and solute transport parameters for each water table depth lysimeter.

Lysimeter	Depth (m)	θ_r ($cm^3\ cm^{-3}$)	θ_s ($cm^3\ cm^{-3}$)	α (cm^{-1})	η (-)	K_s ($cm\ d^{-1}$)	$\curlyvee$ (-)	λ (cm)
WTD= 1.25 m	0.0–0.4	0.067	0.435	0.013	2.51	400.0	0.5	50.0
	0.4–2.35	0.067	0.435	0.023	1.50	30.0	0.5	150.0
	2.35–2.6	0.045	0.435	0.145	2.68	712.8	0.5	30.0
WTD= 1.5 m	0.0–0.4	0.067	0.435	0.009	3.00	400.0	0.5	50.0
	0.4–2.35	0.067	0.435	0.018	1.60	28.0	0.5	150.0
	2.35–2.6	0.045	0.435	0.145	2.68	712.8	0.5	30.0
WTD= 2.0 m	0.0–0.4	0.067	0.435	0.008	2.45	400.0	0.5	50.0
	0.4–2.35	0.067	0.435	0.014	1.63	20.0	0.5	150.0
	2.35–2.6	0.045	0.435	0.145	2.68	712.8	0.5	30.0
WTD= 2.25 m	0.0–0.4	0.067	0.435	0.007	2.54	400.0	0.5	50.0
	0.4–2.35	0.067	0.435	0.015	1.51	30.0	0.5	150.0
	2.35–2.6	0.045	0.435	0.145	2.68	712.8	0.5	30.0

Note: θ_r and θ_s, residual and saturated water contents, respectively; α and η, empirical shape parameters; K_s, saturated hydraulic conductivity; $\curlyvee$, pore connectivity/tortuosity parameter; λ, soil dispersivity; WTD, water table depth.

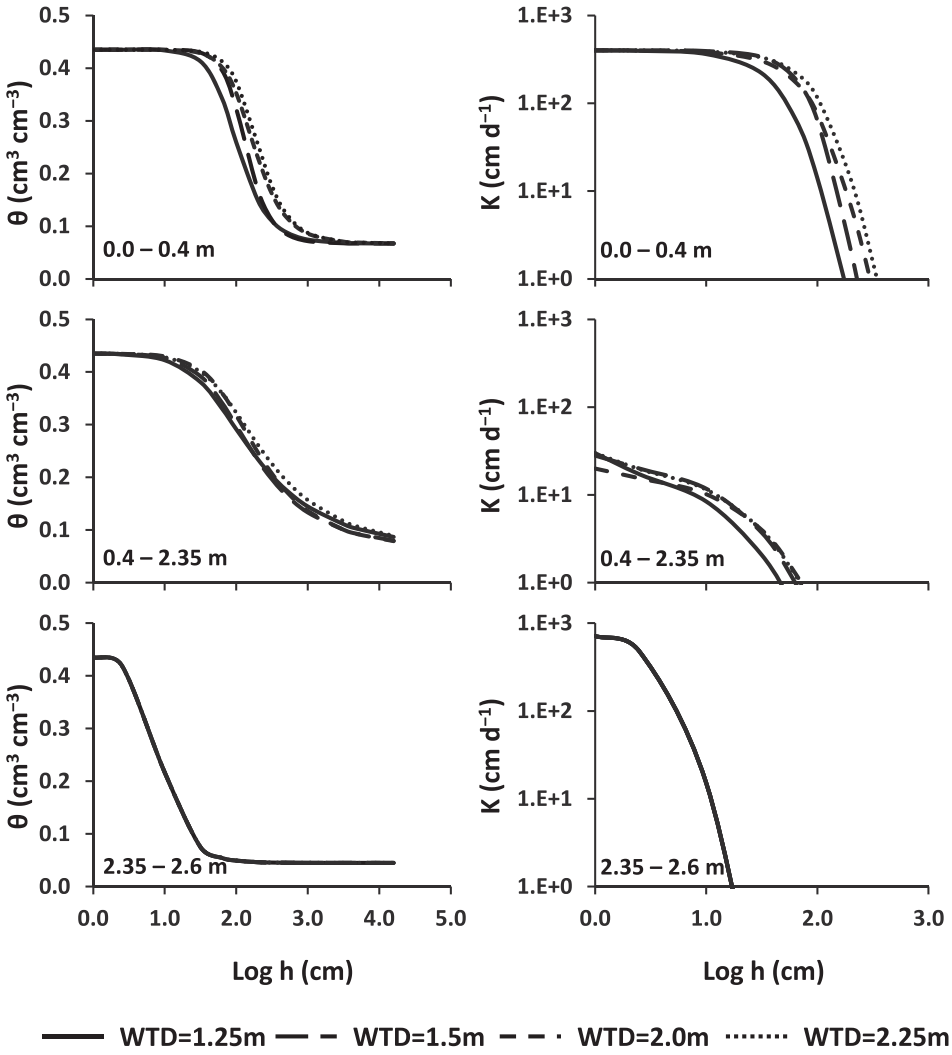

Fig. 2. Soil water retention, θ(h), and soil hydraulic conductivity, K(h), curves in different soil layers of each lysimeter (WTD, water table depth).

coefficients b_0 were all close to the 1.0 target, ranging from 0.969 (WTD=2.25 m) to 0.997 (WTD=2.0 m), indicating that the simulated values were close to the observed ones. The values of R^2 were all greater than 0.752 (WTD=2.25 m), showing that generally, the model could explain most of the variance of the observed data. The errors of the estimates were always small, with RMSE$\leq$ 0.033 $cm^3\ cm^{-3}$ and NRMSE$\leq$ 10.2%. The PBIAS values were also quite small ($-0.357 \leq$PBIAS$\leq$2.111%), with no particular over- or under-estimation tendency when simulating the measured data. Lastly, the NSE values were all greater than 0.742, thus indicating that the variance

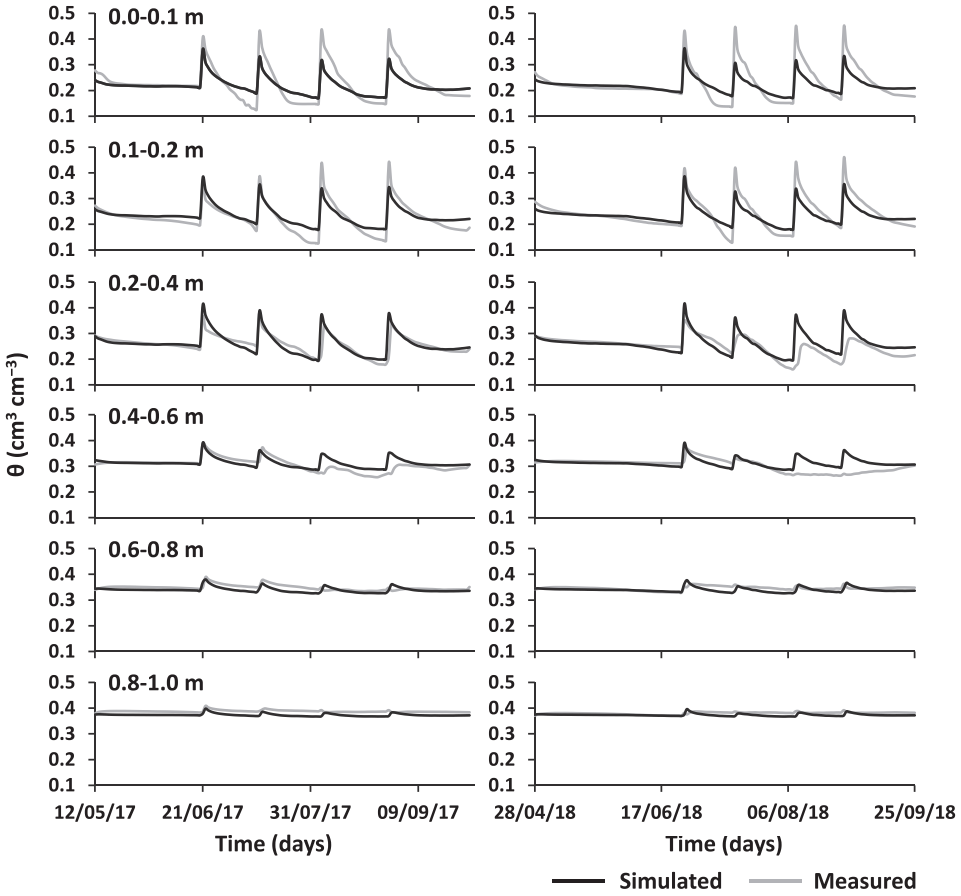

Fig. 3. Measured and simulated soil water contents (θ) at different depths in the lysimeter with water table depth set at 1.25 m during the 2017 (left) and 2018 (right) growing seasons.

of the residuals was largely smaller than the measured data variance. For the 2017 validation season, the goodness-of-fit indicators showed generally the same tendency and a similar range of values as observed for calibration, thus indicating a very good reproduction of measured soil water content values in all lysimeters. The goodness-of-fit indicators were comparable to other Hydrus-1D applications using inverse modeling of soil moisture data (e.g., González et al., 2015; Diongue et al., 2022; Kumar et al., 2022; Ramos et al., 2023), and to the values simulated by the SIMDualKc model for the same lysimeters (Liu et al., 2022b).

3.2.2. *Upward fluxes*

Fig. 4 shows the upward fluxes measured in the unsaturated/saturated interface of each lysimeter as well as the corresponding HYDRUS-1D simulations. In all lysimeters, the upward fluxes from the groundwater table increased after sowing and between irrigation events as the topsoil layers dried up and soil matric heads were reduced. During and immediately after irrigation events, all upward fluxes ceased because then infiltration became the dominant process in the soil. The shallower the groundwater depth, the greater the upward fluxes. The HYDRUS-1D model was able to adequately simulate this dynamic in all lysimeters (Table 5). The worst goodness-of-fit indicators relative to the upward fluxes were obtained for the lysimeter with the deepest water table depth (WTD=2.25 m), where the $R^2 \leq 0.591$, and the NSE ≤ 0.550. Nevertheless, all other indicators were comparable to those computed for other lysimeters, namely the b_o and PBIAS which continued showing good accuracy in simulating the measured data. Statistics were also comparable to Luo and Sophocleous (2010), who estimated groundwater contribution to winter wheat water requirements in the Shandong Province, China, using lysimeter data and the HYDRUS-1D model. Present results were also comparable to those obtained with SIMDualKc when simulating observed upward fluxes with the same and with weighing lysimeters (Liu et al., 2022a, 2022b).

3.2.3. *Deep percolation*

The simulated and measured downward fluxes in the unsaturated/saturated interface of each lysimeter are shown in Fig. 5. Deep percolation was only observed immediately after irrigation events, reducing to null values in the days that followed. The lower the WTD, the smaller the flow peak. HYDRUS-1D was not able to reproduce flow peaks in the lysimeters with the shallowest WTD (WTD≤1.5 m). Measured flow peaks may likely be attributed to preferential flow patches that formed possibly because of soil sampling for determination of the EC_e. A more complex modeling approach would be needed to eventually reach those flow peaks since the current simulations only considered fluxes in the soil matrix (Šimůnek et al., 2003). However, those preferential flow patches were not of natural occurrence to justify that and had little impact on simulations. The goodness-of-fit indicators for the shallower lysimeters were quite acceptable, returning R^2 values ranging from 0.574 to 0.749 and NSE values from 0.468 to 0.748 (Table 5). The same cannot be said for the lysimeters with deeper WTD, which statistical indicators were poor mostly because the majority of the pairwise measured and simulated values were null. A visual analysis of results can only lead to the conclusion that simulations well described deep percolation in those lysimeters.

3.2.4. *Soil salinity*

The EC_e values measured in each lysimeter showed a tendency to

Table 5
Goodness-of-fit for the comparison of measured and simulated soil water contents, upward fluxes, deep percolation, electrical conductivity of the saturation paste extract (EC_e), and actual crop evapotranspiration ($ET_{c\ act}$). Calibration and validation were performed with the 2018 and 2017 datasets, respectively.

Statistics	WTD= 1.25 m		WTD= 1.5 m		WTD= 2.0 m		WTD= 2.25 m	
	2017	2018	2017	2018	2017	2018	2017	2018
Soil water contents								
b_0	0.989	0.992	0.997	0.997	0.982	0.997	0.943	0.969
R^2	0.940	0.893	0.894	0.894	0.798	0.784	0.826	0.752
RMSE ($cm^3\ cm^{-3}$)	0.021	0.025	0.024	0.025	0.033	0.033	0.031	0.033
NRMSE (%)	6.6	8.1	7.4	7.7	10.2	10.6	9.7	10.8
PBIAS (%)	0.51	0.07	0.00	-0.36	1.59	-0.35	5.36	2.11
NSE	0.938	0.893	0.893	0.893	0.772	0.774	0.750	0.742
Upward fluxes								
b_0	1.019	0.853	1.217	1.013	1.063	0.866	1.021	0.771
R^2	0.859	0.814	0.796	0.857	0.591	0.574	0.479	0.591
RMSE (mm)	0.387	0.480	0.469	0.327	0.384	0.354	0.338	0.259
NRMSE (%)	36.0	42.6	67.9	42.9	87.5	69.3	111.9	75.6
PBIAS (%)	0.28	17.35	-27.38	2.66	-18.87	11.80	-29.33	14.87
NSE	0.817	0.769	0.556	0.811	0.337	0.429	0.157	0.550
Deep percolation								
b_0	0.848	0.779	0.829	0.959	0.812	1.800	0.238	1.517
R^2	0.574	0.749	0.604	0.669	0.432	0.519	0.055	0.262
RMSE (mm)	1.287	0.929	1.014	0.731	0.677	0.275	0.978	0.158
NRMSE (%)	267.7	194.2	196.6	234.1	318.0	745.5	606.4	1558.0
PBIAS (%)	-33.28	-11.29	1.72	-32.18	-22.54	-184.43	-50.11	-294.63
NSE	0.468	0.748	0.538	0.566	0.180	-2.491	-0.234	-5.081
EC_e								
b_0	0.914	0.990	0.961	1.067	1.021	1.091	1.117	1.121
R^2	0.384	0.432	0.328	0.381	0.361	0.429	0.635	0.611
RMSE ($dS\ m^{-1}$)	1.128	1.182	1.013	1.080	0.831	0.889	0.609	0.610
NRMSE (%)	26.7	29.6	26.3	29.0	24.9	27.1	19.7	20.1
PBIAS (%)	2.12	-7.78	-2.06	-13.56	-5.77	-12.88	-12.50	-13.38
NSE	0.375	0.378	0.318	0.203	0.217	0.132	0.146	0.127
$ET_{c\ act}$								
b_0	0.857	0.878	0.912	0.954	0.817	0.693	0.855	0.712
R^2	0.856	0.807	0.807	0.825	0.824	0.933	0.794	0.897
RMSE ($mm\ d^{-1}$)	0.924	0.950	0.913	0.754	1.109	1.544	0.997	1.450
NRMSE (%)	28.1	31.2	30.1	26.5	32.5	38.1	29.7	38.4
PBIAS (%)	10.59	7.67	3.68	3.35	15.10	31.42	14.06	26.39
NSE	0.823	0.793	0.804	0.810	0.765	0.617	0.730	0.684

Note: b_0, regression coefficient; R^2, coefficient of determination; RMSE, root mean square error; NRMSE, ratio of the RMSE to the mean of observed data; PBIAS, percent bias; NSE, model efficiency; WTD, water table depth.

increase over each growing season. The salinity levels were greater in the lysimeter with the shallowest water table (WTD=1.25 m) (Fig. 6), in which topsoil layer (0.0–0.1 m) registered the highest EC_e values (6.0–9.23 $dS\ m^{-1}$), and in the bottom layer (1.0–1.2 m) the lowest (1.94–3.60 $dS\ m^{-1}$). On the opposite, the salinity levels were lower in the lysimeter with WTD= 2.25 m, which topsoil layer (0.0–0.1 m) showed EC_e values only ranging from 2.78 to 6.08 $dS\ m^{-1}$, and the bottom values (1.8–2.0 m) from 2.16 to 2.79 $dS\ m^{-1}$. The autumn irrigation always caused a drop in the EC_e values in the soil profile in every lysimeter.

The goodness-of-fit indicators between measured and simulated EC_e values were less good than those relative to soil moisture and upward fluxes (Table 5). This was expected as statistical indicators for solute transport simulations are usually worse than for soil moisture because they are dependent on (i) soil moisture simulations; (ii) the established relation for converting measured values of $EC_{1:5}$ into EC_e data, which is obviously subjected to error; and (iii) the assumed relationship for converting simulated EC_{sw} into EC_e data, which is also subjected to uncertainty (Skaggs et al., 2006). As a result, the R^2 values ranged from 0.33 to 0.64, thus denoting a somewhat wide dispersion of values along the regression line, and the NSE values from 0.13 to 0.38, nevertheless positive and indicating that the variance of residuals was smaller than the variance of observations. The values for b_0 were generally 10% close to 1.0, indicating under-estimation for small WTD and over-estimation when WTD was large, with best results for WTD around 1.5 m. The NRMSE values were relatively low (19.7%≤NRMSE≤29.0), and comparable to Ramos et al. (2023) who conducted a similar validation approach based on EC_e data.

3.2.5. Actual evapotranspiration

The $ET_{c\ act}$ values increased during the development stage, and reached maximum values above 8 mm d^{-1} at the beginning of August during the mid-season stage in both seasons, to drop again with senescence in the late-season stage until maize was harvested at the end of September (Fig. 7). In all crop stages, $ET_{c\ act}$ values never reached the potential ET_c values because of the combined effects of water and salinity stresses on root water uptake. The HYDRUS-1D model was able to simulate $ET_{c\ act}$ values very well, either during the calibration or the validation, with R^2 values from 0.794 to 0.933 and NSE values from 0.617 to 0.823 (Table 5). For these results, the activation of the compensation mechanism was decisive (Šimůnek and Hopmans, 2009). However, some underestimation of $ET_{c\ act}$ values was noticed in lysimeters with WTD= 2.0 and WTD= 2.25 during the 2018 growing season, with b_0 values dropping to 0.693 and 0.712, respectively, and PBIAS increasing to values above 31% and 26%, respectively. This divergence was more notorious for a short period between July 22nd and July 31st. Because in that period, which followed the irrigation event performed on July 16th, the soil should be drying up and the water and salinity stresses increasing (the next irrigation was only on August 9th), the model predictions seem more realistic than measurement values that were maintained at very high rates. During validation, such problem was not observed, even if b_0 failed to go above values of 0.855. Luo and Sophocleous (2010) also reported similar good statistics for the $ET_{c\ act}$ in their lysimeter study. Er-Raki et al. (2021) showed comparable good estimations of the $ET_{c\ act}$ of winter wheat grown in Morocco using the HYDRUS-1D model. Nevertheless, the goodness-of-fit values previously obtained with SIMDualKc (Liu et al., 2022a, 2022b) were comparable or

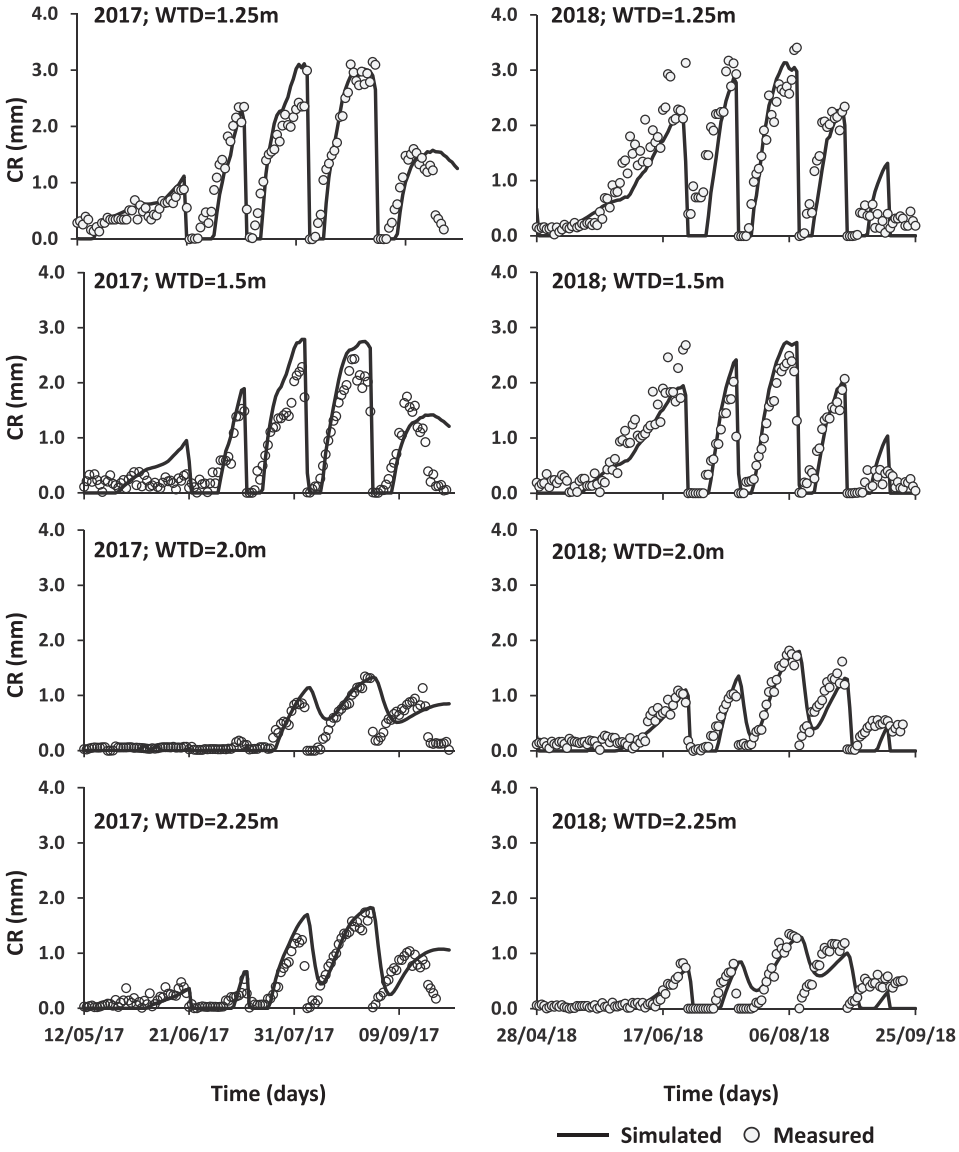

Fig. 4. Measured and simulated capillary rise (upward fluxes) in the unsaturated/saturated interface of each lysimeter during the 2017 (left) and 2018 (right) growing seasons (CR, capillary rise; WTD, water table depth).

superior.

3.3. Soil water balance

The components of the soil water balance estimated by the HYDRUS-1D model for each lysimeter and crop season are given in Table 6, including the non-growing period. Vertical fluxes were computed at 1.25 m depth to facilitate the comparison between lysimeters. During crop seasons, the $T_{c\ act}$ was very similar between lysimeters, with seasonal cumulative values slightly lower in 2017 (396–401 mm) than in 2018 (413–424 mm). In all lysimeters, potential root water uptake was reduced 24–25% in 2017 and 25–27% in 2018 due to water and salinity stresses. The effect of groundwater depth on the $T_{c\ act}$ was thus only minor. A direct comparison to Liu et al. (2022b) needs to consider that their results were obtained using the SIMDualKc model, which follows a semi-empirical approach. Still, in their study, potential root water uptake was reduced by 25% (2017) and 23% (2018) in the lysimeter with the shallowest groundwater depth (WTD=1.25 m), which was the most affected by salinity stress. The lysimeters with the deepest water table (WTD=2.25 m) and less afflicted by salinity showed root water uptake reductions of only 16% (2017) and 17% (2018).

Because the SIMDualKc approach for computing the salinity stress is directly based on the measured EC_e values (Pereira et al., 2007; Minhas et al., 2020), root water uptake reductions agreed with the salinity levels monitored in each lysimeter. This was not verified using the HYDRUS-1D model mostly because the approach adopted considered the EC_{sw} instead, which was modeled as a non-reactive tracer (values were then converted to the EC_e for comparison). Likely, only by using the ion chemistry module also available in HYDRUS-1D, which considers the transport of soluble ions and reactions between the liquid and solid phases (Gonçalves et al., 2006; Ramos et al., 2011), would be possible to have a clearer distinction of the $T_{c\ act}$ under different soil salinity and groundwater depth conditions.

In addition, the upward fluxes of water into the rootzone were much dependent on the groundwater depth (Table 6), resulting in higher values (151–155 mm) in the lysimeter with WTD= 1.25 m and lower values (56–57 mm) in the lysimeter with WTD= 2.25 m. Hence, the groundwater contribution to the $T_{c\ act}$ ranged from 37% to 38% in the lysimeter with WTD= 1.25 m to 14% in the lysimeter with WTD= 2.25 m, showing a similar trend and close values to Liu et al.

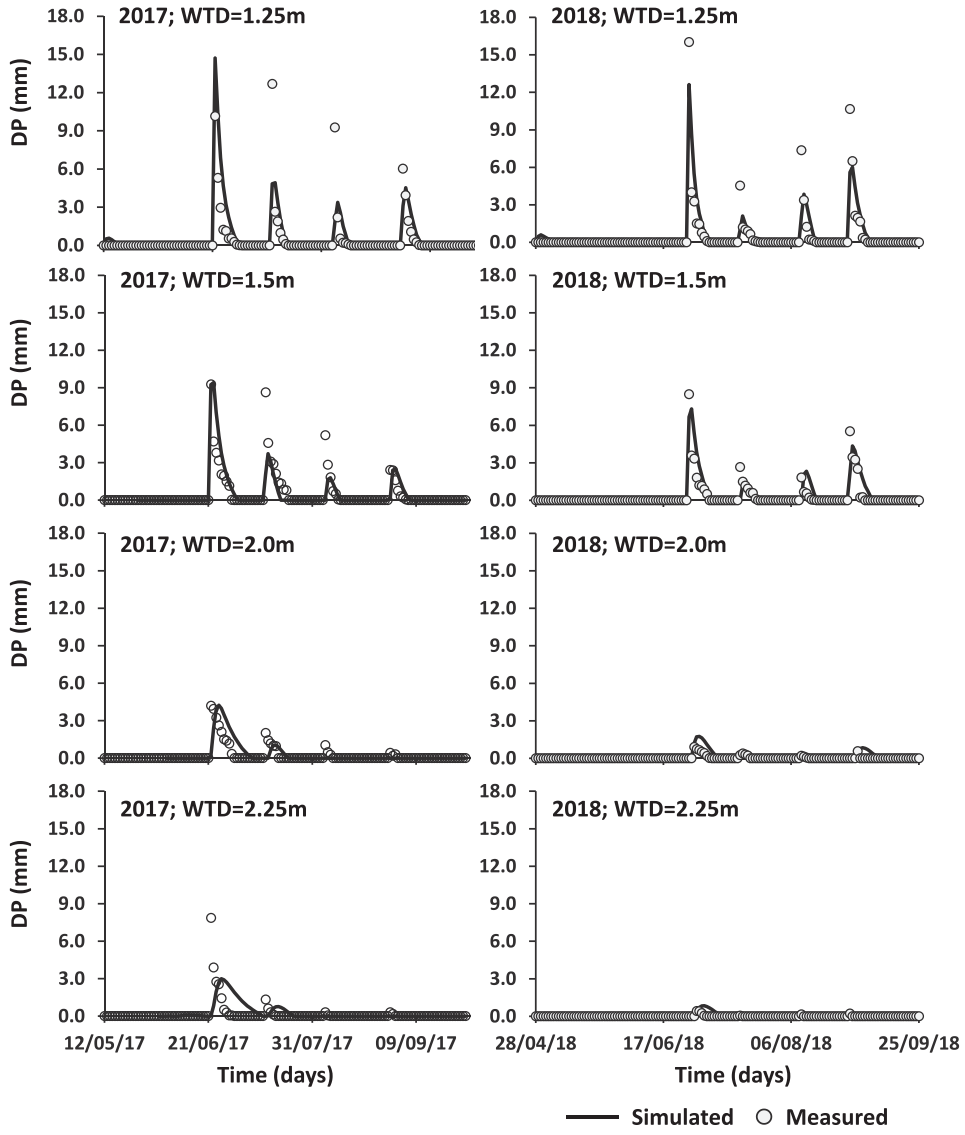

Fig. 5. Measured and simulated deep percolation (DP) in the unsaturated/saturated interface of each lysimeter during the 2017 (left) and 2018 (right) growing seasons (WTD, water table depth).

(2022b). These estimates also agree with available studies aimed at assessing the groundwater contribution to maize water demand under saline conditions in Hetao when using modeling results (e.g., Gao et al., 2015; Ren et al., 2016; Wu et al., 2023).

Percolation values further decreased with groundwater depth, mostly because of the larger drier rootzone layer under such conditions. Nonetheless, estimated values are related to the less efficient irrigation scheduling adopted in the experiment, i.e., with less opportune water applications, which followed traditional practices carried out by local farmers. However, that lower efficiency is beneficial in terms of salt leaching and may be considered desirable. The non-growing period was characterized by high percolation due to the application of 200 mm as autumn irrigation for leaching the accumulated salts during the crop season.

3.4. Salt balance and leaching of salts under diverse autumn irrigation depths

Table 7 presents the salt balance for each lysimeter in both crop seasons. Like for the soil water balance, the salt balance was computed for the growing period and the non-growing period, the latter to appropriately consider the effect of autumn irrigation on salt leaching. The salt balance was also computed for the 0.0–1.25 m soil layer, again to facilitate the comparison between lysimeters.

Salts were added to the soil mainly through the irrigation water (3.76–3.97 tonnes ha^{-1}) during the crop period, through the autumn irrigation (2.24–2.37 tonnes ha^{-1}), as well transported with the capillary rise of saline groundwater. The greater the upward flux, the greater the salinity build-up in the rootzone. This was evidenced in the case of the lysimeter with WTD= 1.25 m, with 3.49–3.57 tonnes ha^{-1} of salts ascending to the rootzone while the lysimeter with WTD= 2.25 m had a salt load via capillary rise of only 1.20 tonnes ha^{-1} during the crop season.

While some percolation existed in all lysimeters during the growing period, which promoted salt leaching and alleviated the salinity stress, the autumn irrigation was fundamental for removing the most substantial part of the salts accumulated in the rootzone during the previous maize season. Nonetheless, leaching from autumn irrigation was greater in the lysimeters with shallower (WTD$\leq$1.5 m; $\geq$6.31 tonnes ha^{-1}) than deeper (WTD$\geq$2.0 m; $\leq$4.75 tonnes ha^{-1}) groundwater levels due to the higher accumulation of salts in these lysimeters and to the higher soil moisture condition of the deeper rootzone layer. The lysimeter with

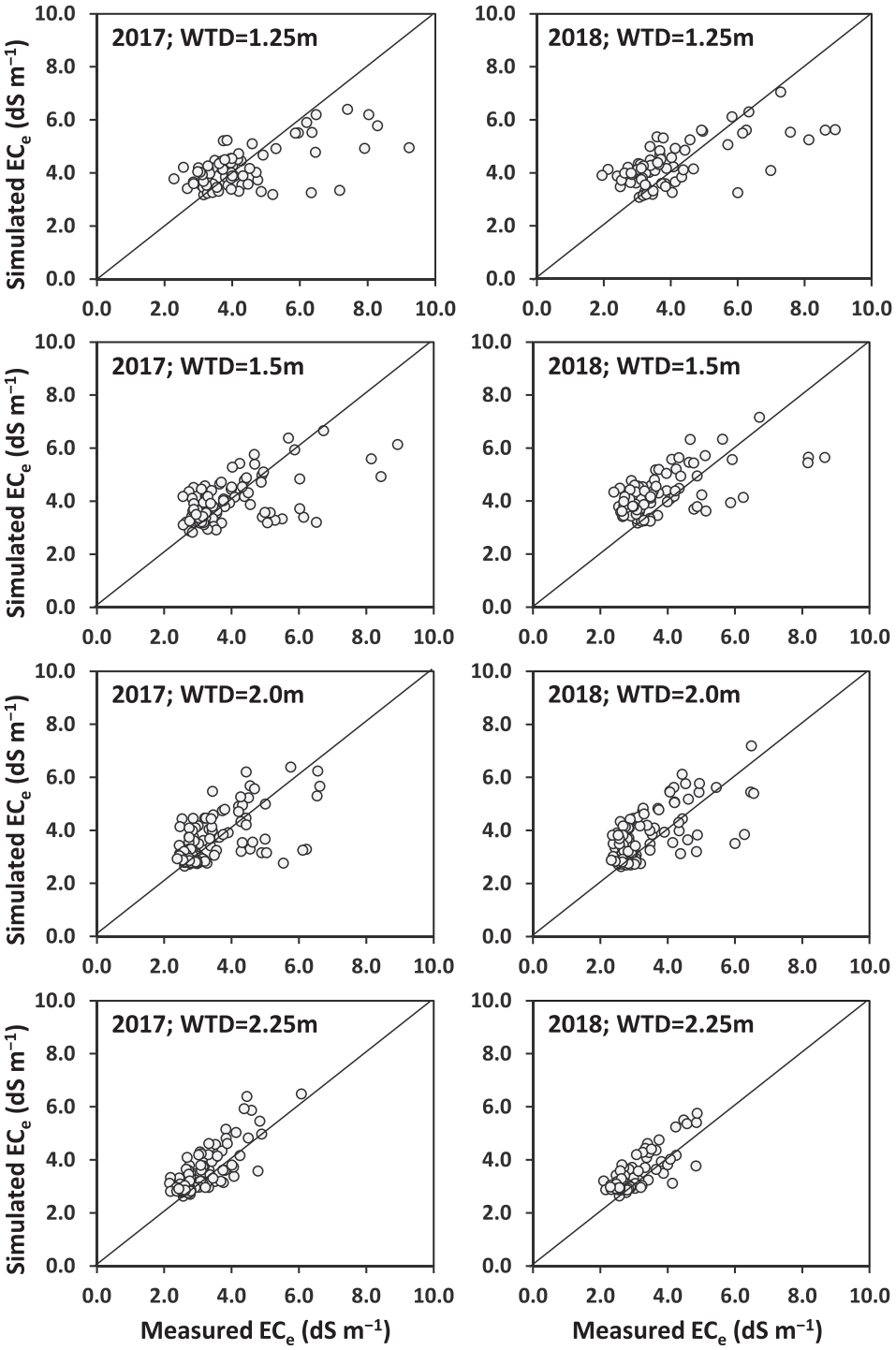

Fig. 6. Scatterplots of the pairwise values of measured and simulated values of the electrical conductivity of the saturation paste extract (EC_e) in each lysimeter during the 2017 (left) and 2018 (right) growing seasons (WTD, water table depth).

WTD= 1.5 m further showed the highest leaching efficiency (83.5–87.5%) compared with the other lysimeters, particularly with the one with WTD= 2.25 m, where the leaching efficiency was the lowest (51.3–53.6%).

The literature already recognizes the autumn irrigation as an important control mechanism for soil salinity in the Hetao irrigation district (Xu et al., 2010; Mao et al., 2017; Wu et al., 2019; Cao et al., 2023). The autumn irrigation is further fundamental for improving the structure of the soil root zone due to the multiple occurrences of soil freezing and thawing, particularly in loess silty soils, and for increasing soil water content for the summer crops to be planted next April, after soil unfreezes (Wang and Akae, 2004; Li et al., 2012; Wang et al., 2020). Yet, the amount of water required for salt leaching, the most adequate irrigation schedule and method, the effectiveness of the procedure, and the relation to groundwater depth is often the source of some debate.

In this study, the leaching efficiency of autumn irrigation in relation to water table depth was explored using the calibrated HYDRUS-1D model. The same water table depths ranging from 1.25 m to 2.25 m were considered as well as irrigation dates. Varying the autumn irrigation depth considerably impacted the effectiveness of the autumn

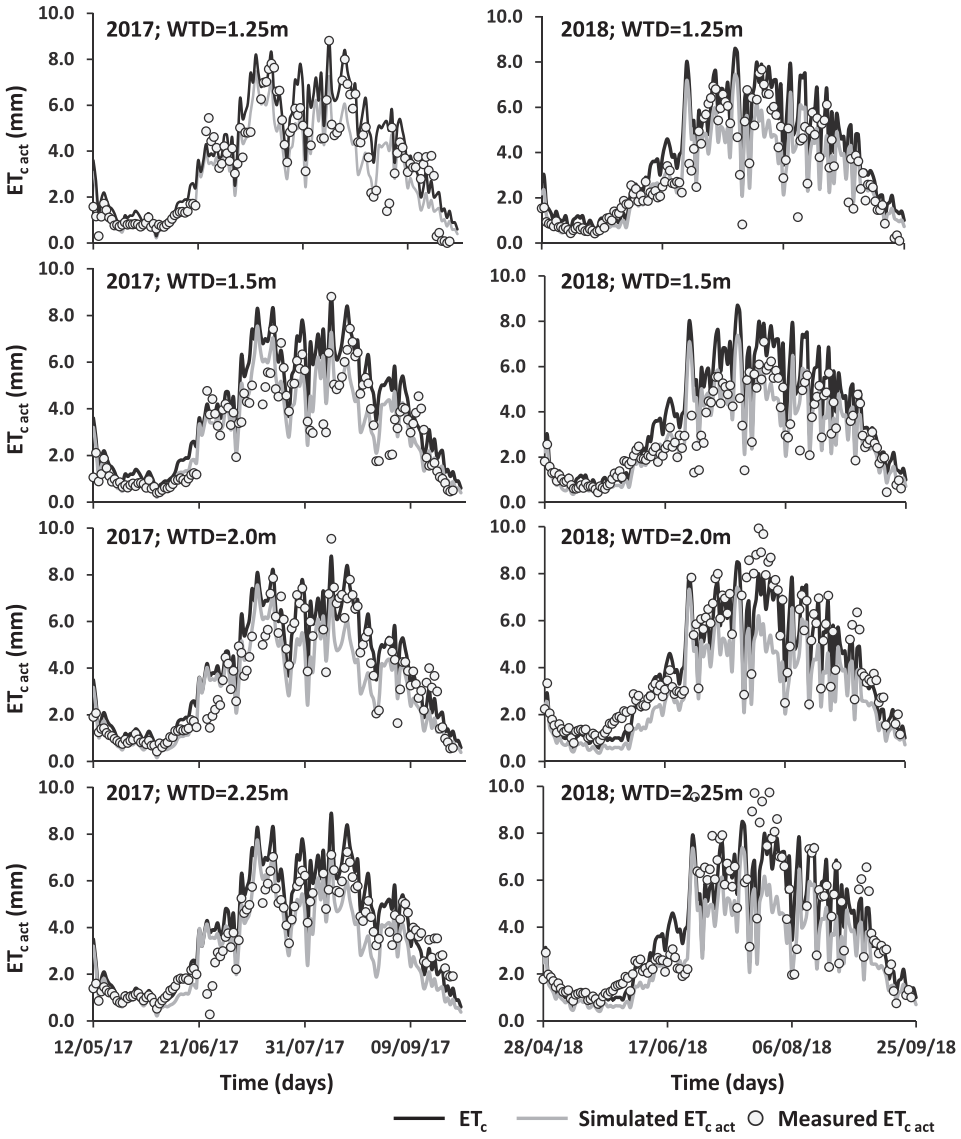

Fig. 7. Dynamics of potential crop evapotranspiration (ET_c) and measured and simulated actual evapotranspiration ($ET_{c\ act}$) in each lysimeter during the 2017 (left) and 2018 (right) growing seasons (WTD, water table depth).

irrigation salinity control measure. Fig. 8 shows the leaching efficiency for each WTD and growing season (2017 and 2018) for autumn irrigation depths ranging from 50 to 400 mm.

The lysimeter with WTD= 1.25 m never showed a higher leaching efficiency than the 78% obtained during experimental conditions (200 mm) regardless of the amount of water applied. Likewise, the lysimeter with WTD= 1.5 m showed the highest leaching efficiency (83.5–87.5%) for an autumn irrigation depth of 200 mm. In both these lysimeters, higher depths were never as effective due to the additional salt load to the rootzone and poor drainage conditions. These results agree with the discussion by Minhas et al. (2020) about the ineffectiveness of leaching in the presence of shallow and saline water tables unless subsurface drainage is considered.

The lysimeter with WTD= 2.0 m showed the effectiveness of the autumn irrigation increasing from 67% to 68–86% when the autumn irrigation depth increased from 200 to 250 mm. However, higher depths also became ineffective in promoting salt leaching (see Fig. 8). Lastly, the lysimeter with WTD= 2.25 m showed the most favorable drainage conditions, with the effectiveness of autumn irrigation increasing abruptly when small increments above 200 mm were applied. With 220 mm, the leaching efficiency increased from 51% to 54% to 85–91%, i.e., an additional 20 mm of water represented an increase of the leaching efficiency of about 35–40%. With 250 mm (+50 mm), all salts applied during the growing and non-growing seasons were removed. Only with 400 mm, the leaching efficiency dropped again to values below 100%. The referred irrigation depths (220 and 250 mm) are only slightly lower than the 270 mm recommended by Chang et al. (2019) for effective salt leaching when the groundwater level was at 2.0 m depth or shallower. Results confirm the considerations by Mao et al. (2017) referring that the key to controlling soil salinity in the rootzone would be through increasing the amount of autumn irrigation water or decreasing the groundwater level to reduce the salt input due to the capillary rise; however, related thresholds were not proposed.

The results in Fig. 8 contradict those by Liu et al. (2022c), who found a negative relationship between the depth of the water table and the autumn irrigation depth using an empirical water and salt balance model. In fact, these authors propose the highest application depth for the smaller WTD, and vice-versa, contrarily to lysimeter observations and HYDRUS-1D simulations. Similarly, Sun et al. (2019) recommended a decrease in autumn irrigation requirements when WTD increases, and an increase in autumn irrigation depth with the increase in groundwater salinity. These authors used a simplified water and mass balance model,

Table 6
Soil water balance terms in all lysimeters during the 2017 and 2018 seasons.

Lysimeters	I (mm)	P (mm)	CR (mm)	ΔSW (mm)	T_c (mm)	$T_{c\ act}$ (mm)	E_s (mm)	DP (mm)	RO (mm)
Crop season 2017									
WTD= 1.25 m	336	0	151	29	528	401	26	90	0
WTD= 1.5 m	336	0	124	45	528	400	25	81	0
WTD= 2.0 m	336	0	78	72	528	400	22	63	0
WTD= 2.25 m	336	0	56	90	528	396	25	61	0
Non-growing period 2017									
WTD= 1.25 m	200	20	39	87	7	0	79	267	0
WTD= 1.5 m	200	20	34	108	7	0	75	287	0
WTD= 2.0 m	200	20	26	34	7	0	69	211	0
WTD= 2.25 m	200	20	22	-38	7	0	65	138	0
Crop season 2018									
WTD= 1.25 m	336	0	155	32	566	424	18	80	0
WTD= 1.5 m	336	0	125	48	566	413	21	76	0
WTD= 2.0 m	336	0	75	70	566	419	19	42	0
WTD= 2.25 m	336	0	57	84	566	418	19	40	0
Non-growing period 2018									
WTD= 1.25 m	200	11	45	85	7	0	72	269	0
WTD= 1.5 m	200	11	41	106	7	0	70	288	0
WTD= 2.0 m	200	11	28	45	7	0	65	219	0
WTD= 2.25 m	200	11	21	-18	7	0	61	153	0

Note: I, irrigation; P, precipitation; CR, capillary rise; ΔSW, soil water storage variation; T_c, potential crop transpiration; $T_{c\ act}$, actual crop transpiration; E_s, soil evaporation; DP, deep percolation; RO, runoff; WTD, water table depth.

Table 7
Salt balance in the top 1.25 m layer of each lysimeter during the 2017 and 2018 seasons.

Salt loads (tonnes ha^{-1})	WTD= 1.25 m		WTD= 1.5 m		WTD= 2.0 m		WTD= 2.25 m	
	2017	2018	2017	2018	2017	2018	2017	2018
Crop season:								
I	3.98	3.76	3.98	3.76	3.97	3.76	3.97	3.76
P	0.00	0.00	0.00	0.00	0.00	0.00	0.00	0.00
CR	3.49	3.47	2.75	2.92	1.61	1.53	1.20	1.20
DP	2.00	1.84	1.69	1.76	1.17	0.80	1.18	0.76
Balance	5.47	5.40	5.04	4.92	4.41	4.49	4.00	4.20
Non-growing period:								
I	2.37	2.24	2.37	2.24	2.37	2.24	2.37	2.24
P	0.01	0.01	0.01	0.01	0.01	0.01	0.01	0.01
CR	0.96	1.09	0.80	1.03	0.59	0.63	0.50	0.48
DP	6.40	6.31	6.58	6.98	4.55	4.75	2.95	3.36
Balance	− 3.07	− 2.97	− 3.40	− 3.70	− 1.58	− 1.87	− 0.07	− 063
Final balance:	**2.40**	**2.42**	**1.64**	**1.22**	**2.83**	**2.63**	**3.92**	**3.57**
Leaching Efficiency (%)	**77.7**	**77.1**	**83.5**	**87.5**	**66.9**	**67.9**	**51.3**	**53.6**

Note: I, irrigation; P, precipitation; CR, capillary rise; DP, deep percolation; WTD, water table depth.

which predictions were validated through comparison with HYDRUS-1D simulations instead of field data. Again, the results in Fig. 8 suggest a more complex relationship between the controlling factors of soil salinity than the simple linear relations reported by Liu et al. (2022c) and Sun et al. (2019).

All lysimeters showed decreasing leaching efficiencies when reducing the autumn irrigation depth below 200 mm (Fig. 8). This directly agrees with Cao et al. (2023), who conducted a scenario analysis using a Hydro-agro-economic optimization model, revealing an increase of soil salt storage in the root zone as winter irrigation depth was reduced. The direct effects of decreasing autumn irrigation application depths were land fallow, increased soil salinity, and decreased agriculture revenues in the Hetao. Chang et al. (2019), using the DrainMod model, also estimated an increase in soil salinity in Hetao when the autumn irrigation depth was reduced. Liu et al. (2022c) further reported increased soil salinization in Hetao's irrigated areas as the autumn irrigation decreased. Therefore, water savings in the Hetao irrigation district at expense of the autumn irrigation need to carefully consider the consequences in terms of land degradation and consequent economic losses for farmers. In this sense, Cao et al. (2023) further advert to the need of considering the trade-off between the loss of benefits from reducing winter irrigation in Hetao and the new benefit that the saved winter irrigation could generate elsewhere. However, the uncertainty of such type of calculations has to be very carefully evaluated.

In the companion paper (Liu et al., 2022b) is concluded that the best cropping conditions (higher crop height, leaf area index, and yield) and lower salinity levels were found in the lysimeter with WTD= 2.0 m because shallower water table depths always induced a larger accumulation of salts in the root zone due to higher upward water fluxes. In the current study, modeling results showed that the lysimeter with WTD= 1.5 m was the one where the autumn irrigation of 200 mm was more effective in leaching salts away from the rootzone layer. This is likely related to the commonly adopted application depth used in Hetao, which led to adopting 200 mm in the lysimeters experiments (Liu et al., 2020a, b). However, simulating larger autumn irrigation depths with the lysimeters with WTD= 2.0 m and WTD= 2.25 m led to comparable or even better conditions for salt control. These results are in favor of the progressive installation of drainage in the Hetao plain. Because groundwater fluxes to the rootzone are also important to fulfil crop water needs, a WTD= 2.0 m may be the best compromise between crop growth and salinity control, in agreement with results by Liu et al. (2022b). Nonetheless, more efficient irrigation schedules should be developed, combined with the appropriate setting of the water table depth, to improve the effectiveness of salt leaching in the Hetao region.

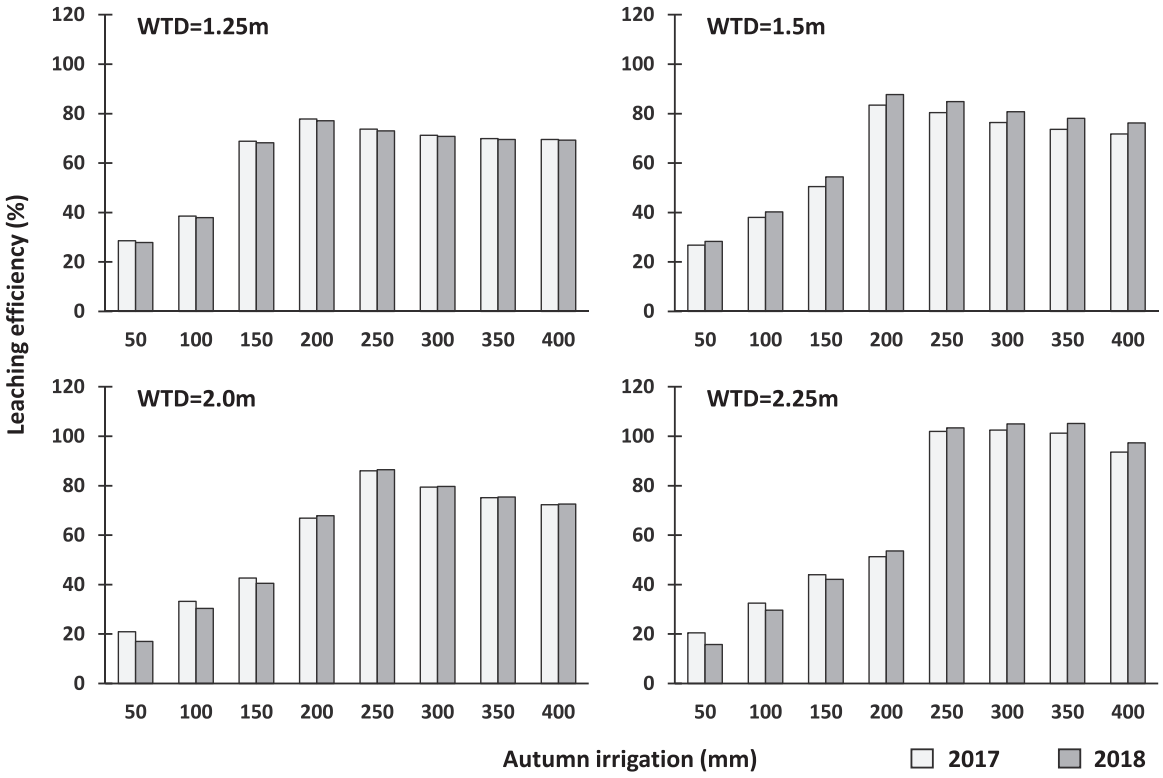

Fig. 8. The efficiency of autumn irrigation depth for leaching rootzone salts under variable water table depth (WTD) conditions.

An example is given by Wu et al. (2019), where the anticipation of the autumn irrigation date by 10 days, combined with a longer application period, allowed reducing irrigation water by 20%, controlling the groundwater level, and minimizing soil salinization problems. However, on the one hand, it is not yet clear how to adopt this in practice and, on the other hand, how to apply large irrigation depths when drip irrigation would be adopted. Currently, the progressive use of drip systems in Hetao is apparently concurrent with the application of the autumn irrigation, which area has remained stable over the last decade (Qian et al., 2022). Moreover, subsurface drainage, now being installed, require new irrigation approaches to maximize its impact in improving salt leaching.

4. Conclusions

This study used two sets of five static water-table lysimeters, which fixed depths ranged from 1.25 to 2.25 m, over two growing seasons. The HYDRUS-1D model was used to simulate soil water contents, capillary fluxes, DP, EC_e, and $ET_{c\ act}$ data measured in each lysimeter. This constituted one of the most extensive evaluations of the different components of the soil water balance ever performed with this model. The model was able to well reproduce soil water contents data and $ET_{c\ act}$. The upward capillary fluxes and DP were also well simulated but the EC_e simulation was less good but acceptable.

In every lysimeter, irrigation was by flooding and followed standard management performed by local farmers. The water was conveyed from the saline groundwater and delivered to the lysimeters. As such, root water uptake was much impacted by water stress and soil salinity levels, with reductions reaching 24–27%, which largely affected yields. The influence of water table depth on root water uptake was only minor. On the other hand, the upward fluxes to the rootzone layer were much influenced by the groundwater depth, with greater values found with shallower water tables.

Salts were mobilized to the rootzone mostly with irrigation and by capillary rise. Results lead to conclude that the shallower the groundwater depth, the greater the salinity build-up in the rootzone over the crop season. The autumn leaching irrigation, which is performed in Hetao since ancient times, was the most important mechanism for controlling soil salinity levels in the rootzone. Its efficiency was also mostly associated with groundwater depth, with the greatest efficiency values (83.5–87.5%) observed for the lysimeter with WTD= 1.5 m. However, when increasing the autumn irrigation depth from 200 to 220 or 250 mm, the lysimeters with WTD= 2.0 m and WTD= 2.25 m showed comparable or even higher efficiencies (85–100%), thus evidencing better vertical drainage conditions and allowing to consider the adoption of such irrigation depths for autumn irrigation when further searching the best WTD conditions.

Because the characteristics of autumn irrigation are hardly compatible with the characteristics of modern irrigation systems such as drip, the transition of irrigation methods currently in place in Hetao, and in other places of the world also affected by salinization problems, needs to consider developing new approaches to satisfy the needs relative to leaching and soil protection. This study shows that for deeper WTD, soil salinization in Hetao can be controlled with autumn irrigation depths of 220–250 mm. However, for shallower WTD, the effectiveness of autumn irrigation is to be known in the long-term, and new solutions are required. Developing new approaches to the autumn leaching and improving silty soils' structural conditions while progressively adopting drip irrigation should be imperative to the sustainability of local production systems and, therefore, a main research issue.

Declaration of Competing Interest

The authors declare that they have no known competing financial interests or personal relationships that could have appeared to influence the work reported in this paper.

Data availability

The data that has been used is confidential.

Acknowledgments

This work was funded by national funds through FCT – Fundação para a Ciência e a Tecnologia, I.P., under projects UIDP/EEA/50009/2020 of LARSyS and UIDB/04129/2020 of LEAF-Linking Landscape, Environment, Agriculture and Food Research Center. The study was further supported by the FCT (project HYDROVAR: 2022.03921.PTDC), the National Natural Science Foundation of China (grant number: 52269014), and the National Key Research and Development Program of the Chinese Ministry of Science and Technology (grant number: 2021YFD1900602–6). The support of FCT through grant attributed to T. B. Ramos (CEECIND/01152/2017) and to P. Paredes (DL57/2016/CP1382/CT0022) are also acknowledged.

References

Allen, R.G., Howell, T.A., Pruitt, W.O., Walter, I.A., Jensen, M.E., 1991a. Lysimeters for evapotranspiration and environmental measurements. In: Proc. Int. Symp. Lysimetry. ASCE, New York, NY.

Allen, R.G., Pruitt, W.O., Jensen, M.E., 1991b. Environmental requirements of lysimeters. In: Allen, R.G., Howell, T.A., Pruitt, W.O., Walter, I.A., Jensen, M.E. (Eds.), Lysimeters for Evapotranspiration and Environmental Measurements. Proc. Int. Symp. Lysimetry. ASCE, New York, pp. 170–181.

Allen, R.G., Pereira, L.S., Raes, D., Smith, M., 1998. Crop evapotranspiration. guidelines for computing crop water requirements. FAO Irrig. Drain. FAO,, Rome, Italy, p. 300.

Allen, R.G., Pereira, L.S., Smith, M., Raes, D., Wright, J.L., 2005. FAO-56 dual crop coefficient method for estimating evaporation from soil and application extensions. J. Irrig. Drain. Eng. 131 (1), 2–13. https://doi.org/10.1061/(ASCE)0733-9437(2005)131:1(2).

Allen, R.G., Pereira, L.S., Howell, T.A., Jensen, M.E., 2011a. Evapotranspiration information reporting: I. Factors governing measurement accuracy. Agric. Water Manag. 98 (6), 899–920. https://doi.org/10.1016/j.agwat.2010.12.015.

Allen, R.G., Pereira, L.S., Howell, T.A., Jensen, M.E., 2011b. Evapotranspiration information reporting: II. Recommended documentation. Agric. Water Manag. 98 (6), 921–929. https://doi.org/10.1016/j.agwat.2010.12.016.

Bai, L., Cai, J., Liu, Y., Chen, H., Zhang, B., Huang, L., 2017. Responses of field evapotranspiration to the changes of cropping pattern and groundwater depth in large irrigation district of Yellow River basin. Agric. Water Manag. 188, 1–11. https://doi.org/10.1016/j.agwat.2017.03.028.

Bai, M., Xu, D., Li, Y., Pereira, L.S., 2010. Stochastic modeling of basins microtopography: analysis of spatial variability and model testing. Irrig. Sci. 28, 157–172. https://doi.org/10.1007/s00271-009-0169-9.

Bresler, E., McNeal, B.L., Carter, D.L., 1982. Saline and Sodic Soils. Advanced Series in Agricultural Sciences 10. Springe -Verl. Berlim Heide 236.

Cao, Z., Zhu, T., Cai, X., 2023. Hydro-agro-economic optimization for irrigated farming in an arid region: The Hetao Irrigation District, Inner Mongolia. Agric. Water Manag. 277, 108095 https://doi.org/10.1016/j.agwat.2022.108095.

Carsel, R.F., Parrish, R.S., 1988. Developing joint probability distributions of soil water retention characteristics. Water Resour. Res. 24, 755–769. https://doi.org/10.1029/WR024i005p00755.

Chang, X., Gao, Z., Wang, S., Chen, H., 2019. Modelling long-term soil salinity dynamics using saltMod in Hetao Irrigation District, China. Comp. Electron. Agric. 156, 447–458. https://doi.org/10.1016/j.compag.2018.12.005.

Diongue, D.M.L., Roupsard, O., Do, F.C., Stumpp, C., Orange, D., Sow, S., Jourdan, C., Faye, S., 2022. Evaluation of parameterisation approaches for estimating soil hydraulic parameters with HYDRUS-1D in the groundnut basin of Senegal. Hydrol. Sci. J. 67 (15), 2327–2343. https://doi.org/10.1080/02626667.2022.2142474.

Dong, Q., Yang, Y., Zhang, T., Zhou, L., He, J., Chau, H.W., Zou, Y., Feng, H., 2018. Impacts of ridge with plastic mulch-furrow irrigation on soil salinity, spring maize yield and water use efficiency in an arid saline area. Agric. Water Manag. 201, 268–277. https://doi.org/10.1016/j.agwat.2017.12.011.

Er-Raki, S., Ezzahar, J., Merlin, O., Amazirh, A., Ait Hssaine, B., Kharrou, M.H., Khabba, S., Chehbouni, A., 2021. Performance of the HYDRUS-1D model for water balance components assessment of irrigated winter wheat under different water managements in semi-arid region of Morocco. Agric. Water Manag. 244, 106546 https://doi.org/10.1016/j.agwat.2020.106546.

FAO, 2015, Status of the world's soil resources. Main Report. Food and Agriculture Organization of the United Nations and Intergovernmental Technical Panel on Soils. Rome, Italy.

Feddes, R.A., Kowalik, P.J., Zaradny, H., 1978, Simulation of field water use and crop yield. Simulation Monographs Pudoc., Wageningen, The Netherlands.

Gao, X., Huo, Z., Bai, Y., Feng, S., Huang, G., Shi, H., Qu, Z., 2015. Soil salt and groundwater change in flood irrigation field and uncultivated land: a case study based on 4-year field observations. Environ. Earth Sci. 73, 2127–2139. https://doi.org/10.1007/s12665-014-3563-4.

Gonçalves, M.C., Šimůnek, J., Ramos, T.B., Martins, J.C., Neves, M.J., Pires, F.P., 2006. Multicomponent solute transport in soil lysimeters with waters of different quality. Water Resour. Res. 42, W08401. https://doi.org/10.1029/2005WR004802.

González, M.G., Ramos, T.B., Carlesso, R., Paredes, P., Petry, M.T., Martins, J.D., Aires, N.P., Pereira, L.S., 2015. Modelling soil water dynamics of full and deficit drip irrigated maize cultivated under a rain shelter. Biosyst. Eng. 132, 1–18. https://doi.org/10.1016/j.biosystemseng.2015.02.001.

Grismer, M., 1990. Leaching fraction, soil salinity, and drainage efficiency. Calif. Agric. 44 (6), 24–26.

Hoffman, G.J., van Genuchten, M.Th, 1983. Soil properties and efficient water use: Water management for salinity control. In: Taylor, H.M., Jordan, W.R., Sinclair, T.R. (Eds.), Limitations and Efficient Water Use in Crop Production, Am. Soc. Of Agron. Madison, WI, pp. 73–85.

Hoffman, G.J., Shalhevet, J., 2007. Controlling salinity. In: Hoffman, G.J., Evans, R.G., Jensen, M.E., Martin, D.L., Elliot, R.L. (Eds.), Design and Operation of Farm Irrigation Systems, 2nd ed. ASABE, St. Joseph, MI, pp. 160–207.

Hopmans, J.W., Qureshi, A.S., Kisekka, I., Munns, R., Grattan, S.R., Rengasamy, P., Ben-Gal, A., Assouline, S., Javaux, M., Minhas, P.S., Raats, P.A.C., Skaggs, T.H., Wang, G., De Jong van Lier, Q., Jiao, H., Lavado, R.S., Lazarovitch, N., Li, B., Taleisnik, E., 2021. Critical knowledge gaps and research priorities in global soil salinity. Adv. Agron. 169, 1–191. https://doi.org/10.1016/bs.agron.2021.03.001.

Jacques, D., Šimůnek, J., Timmerman, A., Feyen, J., 2002. Calibration of Richards' and convection-dispersion equations to field-scale water flow and solute transport under rainfall conditions. J. Hydrol. 259, 15–31. https://doi.org/10.1016/S0022-1694(01)00591-1.

Jarvis, N.J., 1989. A simple empirical model of root water uptake. J. Hydrol. 107, 57–72. https://doi.org/10.1016/0022-1694(89)90050-4.

Kumar, H., Srivastava, P., Lamba, J., Diamantopoulos, E., Ortiz, B., Morata, G., Takhellambam, B., Bondesan, L., 2022. Site-specific irrigation scheduling using one-layer soil hydraulic properties and inverse modelling. Agric. Water Manag. 273, 107877 https://doi.org/10.1016/j.agwat.2022.107877.

Landsberg, J.J., Fowkes, N.D., 1978. Water movement through plant roots. Ann. Bot. 42, 493–508. https://doi.org/10.1093/oxfordjournals.aob.a085488.

Legates, D., McCabe, G., 1999. Evaluating the use of goodness of fit measures in hydrologic and hydroclimatic model validation. Water Resour. Res. 35, 233–241. https://doi.org/10.1029/1998WR900018.

Li, R., Shi, H., Flerchinger, G.N., Akae, T., Wang, C., 2012. Simulation of freezing and thawing soils in Inner Mongolia Hetao Irrigation District, China. Geoderma 173–174, 28–33.

Liu, M., Shi, H., Paredes, P., Ramos, T.B., Dai, L., Feng, Z., Pereira, L.S., 2022a. Estimating and partitioning maize evapotranspiration as affected by salinity using weighing lysimeters and the SIMDualKc model. Agric. Water Manag. 261, 107362 https://doi.org/10.1016/j.agwat.2021.107362.

Liu, M., Paredes, P., Shi, H., Ramos, T.B., Dou, X., Dai, L., Pereira, L.S., 2022b. Impacts of a shallow saline water table on maize evapotranspiration and groundwater contribution using static water table lysimeters and the dual Kc water balance model SIMDualKc. Agric. Water Manag. 273, 107887 https://doi.org/10.1016/j.agwat.2022.107887.

Liu, Y., Zhu, Y., Mao, W., Sun, G., Han, X., Wu, J., Yang, J., 2022c. Development and application of a water and salt balance model for well-canal conjunctive irrigation in semiarid areas with shallow water tables. Agriculture 12, 399. https://doi.org/10.3390/agriculture12030399.

Luo, Y., Sophocleous, M., 2010. Seasonal groundwater contribution to crop-water use assessed with lysimeter observations and model simulations. J. Hydrol. 389, 325–335. https://doi.org/10.1016/j.jhydrol.2010.06.011.

Ma, W., Mao, Z., Yu, Z., van Mensvoort, M.E.F., Driessen, P.M., 2008. Effects of saline water irrigation on soil salinity and yield of winter wheat–maize in North China Plain. Irrig. Drain. Syst. 22, 3–18. https://doi.org/10.1007/s10795-007-9027-1.

Maas, E.V., 1990. Crop salt tolerance. In: Tanji, K.K. (Ed.), Agricultural Salinity Assessment and Management. Manual Eng. Pract., vol. 71. Am. Soc. of Civ. Eng. Reston, VA, pp. 262–304.

Mao, W., Yang, J., Zhu, Y., Ye, M., Wu, J., 2017. Loosely coupled SaltMod for simulating groundwater and salt dynamics under well-canal conjunctive irrigation in semi-arid areas. In: Agric. Water Manage, 192, pp. 209–220. https://doi.org/10.1016/j.agwat.2017.07.012.

Miao, Q., Shi, H., Gonçalves, J.M., Pereira, L.S., 2015. Field assessment of basin irrigation performance and water saving in Hetao, Yellow River basin: Issues to support irrigation systems modernization. Biosyst. Eng. 136, 102–116. https://doi.org/10.1016/j.biosystemseng.2015.05.010.

Miao, Q., Rosa, R.D., Shi, H., Paredes, P., Zhu, L., Dai, J., Gonçalves, J.M., Pereira, L.S., 2016. Modeling water use, transpiration and soil evaporation of spring wheat-maize and spring wheat-sunflower relay intercropping using the dual crop coefficient approach. Agric. Water Manag. 165, 211–229. https://doi.org/10.1016/j.agwat.2015.10.024.

Miao, Q., Shi, H., Gonçalves, J.M., Pereira, L.S., 2018. Basin irrigation design with multicriteria analysis focusing on water saving and economic returns. Appl. wheat Hetao, Yellow River Basin Water 10, 67. https://doi.org/10.3390/w10010067.

Minhas, P.S., Ramos, T.B., Ben-Gal, A., Pereira, L.S., 2020. Coping with salinity in irrigated agriculture: Crop evapotranspiration and water management issues. Agric. Water Manag. 227, 105832 https://doi.org/10.1016/j.agwat.2019.105832.

Moriasi, D.N., Arnold, J.G., Van Liew, M.W., Bingner, R.L., Harmel, R.D., Veith, T.L., 2007. Model evaluation guidelines for systematic quantification of accuracy in watershed simulations. Trans. ASABE 50, 885–900. https://doi.org/10.13031/2013.23153.

Mualem, Y., 1976. A new model for predicting the hydraulic conductivity of unsaturated porous media. Water Resour. Res. 12, 513–522. https://doi.org/10.1029/WR012i003p00513.

Nash, J.E., Sutcliffe, J.V., 1970. River flow forecasting through conceptual models part I—A discussion of principles. J. Hydrol. 10, 282–290. https://doi.org/10.1016/0022-1694(70)90255-6.

Pereira, L.S., Cai, L.G., Hann, M.J., 2003. Farm water and soil management for improved water use in the North China Plain. Irrig. Drain. 52, 299–317. https://doi.org/10.1002/ird.98.

Pereira, L.S., Gonçalves, J.M., Dong, B., Mao, Z., Fang, S.X., 2007. Assessing basin irrigation and scheduling strategies for saving irrigation water and controlling salinity in the upper Yellow River Basin. China. Agric. Water Manag. 93, 109–122. https://doi.org/10.1016/j.agwat.2007.07.004.

Pereira, L.S., Duarte, E., Fragoso, R., 2014. Water use: recycling and desalination for agriculture. In: van Alfen, N. (Ed.), Encyclopedia of Agriculture and Food Systems, vol. 5. Elsevier, San Diego, pp. 407–424.

Pereira, L.S., Paredes, P., Rodrigues, G.C., Neves, M., 2015. Modeling malt barley water use and evapotranspiration partitioning in two contrasting rainfall years. Assessing AquaCrop and SIMDualKc models. Agric. Water Manage. 159, 239–254. Corrig-.-. : Agric. Water Manag. 163, 408. https://doi.org/10.1016/j.agwat.2015.06.006.

Phogat, V., Pitt, T., Cox, J.W., Šimůnek, J., Skewes, M.A., 2018. Soil water and salinity dynamics under sprinkler irrigated almond exposed to a varied salinity stress at different growth stages. Agric. Water Manag. 201, 70–82. https://doi.org/10.1016/j.agwat.2018.01.018.

Qi, Z., Feng, H., Zhao, Y., Zhang, T., Yang, A., Zhang, Z., 2018. Spatial distribution and simulation of soil moisture and salinity under mulched drip irrigation combined with tillage in an arid saline irrigation district, northwest China. Agric. Water Manag. 201, 219–231. https://doi.org/10.1016/j.agwat.2017.12.032.

Qian, X., Qi, H., Shang, S., Wan, H., Wang, R., 2022. Multi-year mapping of flood autumn irrigation extent and timing in harvested croplands of arid irrigation district. GIScience Remote Sens 59, 1598–1623. https://doi.org/10.1080/15481603.2022.2126342.

Ramos, T.B., Gonçalves, M.C., Martins, J.C., van Genuchten, M.Th, Pires, F.P., 2006. Estimation of soil hydraulic properties from numerical inversion of tension disk infiltrometer data. Vadose Zone J. 5, 684–696. https://doi.org/10.2136/vzj2005.0076.

Ramos, T.B., Šimůnek, J., Gonçalves, M.C., Martins, J.C., Prazeres, A., Castanheira, N.L., Pereira, L.S., 2011. Field evaluation of a multicomponent solute transport model in soils irrigated with saline waters. J. Hydrol. 407, 129–144. https://doi.org/10.1016/j.jhydrol.2011.07.016.

Ramos, T.B., Darouich, H., Oliveira, A.R., Farzamian, M., Monteiro, T., Castanheira, N., Paz, A., Alexandre, C., Gonçalves, M.C., Pereira, L.S., 2023. Water use, soil water balance and soil salinization risks of Mediterranean tree crops in orchards of southern Portugal under current climate variability and issues for salinity control and irrigation management. Agric. Water Manag.

Ren, D., Xu, X., Hao, Y., Huang, G., 2016. Modeling and assessing field irrigation water use in a canal system of Hetao, upper Yellow River basin: Application to maize, sunflower and watermelon. J. Hydrol. 532, 122–139. https://doi.org/10.1016/j.jhydrol.2015.11.040.

Ren, D., Xu, X., Ramos, T.B., Huang, Q., Huo, Z., Huang, G., 2017. Modeling and assessing the function and sustainability of natural patches in salt-affected agro-ecosystems: Application to Tamarisk (Tamarix chinensis Lour.) in Hetao, upper Yellow River basin. J. Hydrol. 552, 490–504. https://doi.org/10.1016/j.jhydrol.2017.04.054.

Rhoades, J.D., Kandiah, A., Mashali, A.M., 1992. The use of saline water for crop production. Irrig. Drain. Pap. 48. FAO,, Rome.

Rosa, R.D., Paredes, P., Rodrigues, G.C., Alves, I., Allen, R.G., Pereira, L.S., 2012. Implementing the dual crop coefficient approach in interactive software. 1. Background and computational strategy. Agric. Water Manag. 103, 8–24. https://doi.org/10.1016/j.agwat.2011.10.013.

Šimunek, J., van Genuchten, M.Th, 1996. Estimating unsaturated soil hydraulic properties from tension disc infiltrometer data by numerical inversion. Water Resour. Res. 32, 2683–2696. https://doi.org/10.1029/96WR01525.

Šimůnek, J., Hopmans, J.W., 2009. Modeling compensated root water and nutrient uptake. Ecol. Modell. 220, 505–521. https://doi.org/10.1016/j.ecolmodel.2008.11.004.

Šimůnek, J., Angulo-Jaramillo, R., Schaap, M.G., Vandervaere, J.P., van Genuchten, M. T., 1998. Using an inverse method to estimate the hydraulic properties of crusted soils from tension disc infiltrometer data. Geoderma 86, 61–81. https://doi.org/10.1016/S0016-7061(98)00035-4.

Šimůnek, J., Jarvis, N.J., van Genuchten, M.Th, Gärdenäs, A., 2003. Review and comparison of models for describing non-equilibrium and preferential flow and transport in the vadose zone. J. Hydrol. 272, 14–35. https://doi.org/10.1016/S0022-1694(02)00252-4.

Šimůnek, J., van Genuchten, M.Th, Šejna, M., 2016. Recent developments and applications of the HYDRUS computer software packages. Vadose Zone J. 15 (7) https://doi.org/10.2136/vzj2016.04.0033.

Skaggs, T.H., Shouse, P.J., Poss, J.A., 2006. Irrigating forage crops with saline waters: 2. Modeling root uptake and drainage. Vadose Zone J. 5, 824–837. https://doi.org/10.2136/vzj2005.0120.

Sun, G., Zhu, Y., Ye, M., Yang, J., Qu, Z., Mao, W., Wu, J., 2019. Development and application of long-term root-zone salt balance model for predicting soil salinity in arid shallow water table area. Agric. Water Manag. 213, 486–498. https://doi.org/10.1016/j.agwat.2018.10.043.

U.S. Salinity Laboratory Staff, 1954, Diagnosis and Improvement of Saline and Alcaly Soils. USDA Handbook 60. Washington, USA.

van Genuchten, M.Th, 1980. A closed form equation for predicting the hydraulic conductivity of unsaturated soils. Soil Sci. Soc. Am. J. 44, 892–898. https://doi.org/10.2136/sssaj1980.03615995004400050002x.

van Genuchten, M.Th., 1987, A numerical model for water and solute movement in and below the root zone. Res. Rep. 121, U.S. Salinity Laboratory, USDA, ARS, Riverside, California.

Vanderborght, J., Vereecken, H., 2007. Review of dispersivities for transport modeling in soils. Vadose Zone J. 6, 29–52. https://doi.org/10.2136/vzj2006.0096.

Wang, L., Akae, T., 2004. Analysis of ground freezing process by unfrozen water content obtained from TDR data in Hetao Irrigation District of China. J. Jpn. Soc. Soil Phys. 98, 11–19.

Wang, X., Wang, C., Wang, X., Huo, Z., 2020. Response of soil compaction to the seasonal freezing-thawing process and the key controlling factors. Geoderma 184, 104247. https://doi.org/10.1016/j.catena.2019.104247.

Wesseling, J.G., Elbers, J.A., Kabat, P., van den Broek, B.J., 1991, SWATRE: Instructions for Input. Report, Winand Staring Center, Wageningen, Netherlands.

Wilcox, L.V., Resch, W.F., 1963. Salt balance and leaching requirements in irrigated lands. USDA Tech. Bul. 1290.

Wright, J.L., 1991. Using weighing lysimeters to develop evapotranspiration crop coefficients. In: Allen, R.G., Howell, T.A., Pruitt, W.O., Walter, I.A., Jensen, M.E. (Eds.), Lysimeters for Evapotranspiration and Environmental Measurements. Proc. Int. Symp. Lysimetry, Honolulu, HI. ASCE, New York, NY, pp. 191–199.

Wu, M., Wu, J., Tan, X., Huang, J., Jansson, P.E., Zhang, W., 2019. Simulation of dynamical interactions between soil freezing/thawing and salinization for improving water management in cold/arid agricultural regions. Geoderma 338, 325–342. https://doi.org/10.1016/j.geoderma.2018.12.022.

Wu, Z., Li, Y., Wang, R., Xu, X., Ren, D., Huang, Q., Xiong, Y., Huang, G., 2023. Evaluation of irrigation water saving and salinity control practices of maize and sunflower in the upper Yellow River basin with an agro-hydrological model based method. Agric. Water Manag. 278, 108157 https://doi.org/10.1016/j.agwat.2023.108157.

Xiong, L., Xu, X., Engel, B., Huang, Q., Huo, Z., Xiong, Y., Han, W., Huang, G., 2021. Modeling agro hydrological processes and analyzing water use in a super-large irrigation district (Hetao) of arid upper Yellow River basin. J. Hydrol. 603, 127014 https://doi.org/10.1016/j.jhydrol.2021.127014.

Xu, X., Huang, G., Qu, Z., Pereira, L.S., 2010. Assessing the groundwater dynamics and predicting impacts of water saving in the Hetao Irrigation District. Yellow River Basin Agric. Water Manag 98, 301–313. https://doi.org/10.1016/j.agwat.2010.08.025.

Xu, X., Huang, G., Qu, Z., Pereira, L.S., 2011. Using MODFLOW and GIS to assess changes in groundwater dynamics in response to water saving measures in irrigation districts of the upper Yellow River basin. Water Resour. Manag. 25 (8), 2035–2059. https://doi.org/10.1007/s11269-011-9793-2.

Xu, X., Huang, G., Sun, C., Pereira, L.S., Ramos, T.B., Huang, Q., Hao, Y., 2013. Assessing the effects of water table depth on water use, soil salinity and wheat yield: Searching for a target depth for irrigated areas in the upper Yellow River basin. Agric. Water Manag. 125, 46–60. https://doi.org/10.1016/j.agwat.2013.04.004.

Xu, X., Sun, C., Qu, Z., Huang, Q., Ramos, T.B., Huang, G., 2015. Groundwater recharge and capillary rise in irrigated areas of the Upper Yellow River basin assessed by an agro-hydrological model. Irrig. Drain. 64, 587–599. https://doi.org/10.1002/ird.1928.

Xue, J., Ren, L., 2017. Assessing water productivity in the Hetao Irrigation District in Inner Mongolia by an agro-hydrological model. Irrig. Sci. 35, 357–382. https://doi.org/10.1007/s00271-017-0542-z.

Yang, T., Šimůnek, J., Mo, M., Mccullough-Sanden, B., Shahrokhnia, H., Cherchian, S., Wu, L., 2019. Assessing salinity leaching efficiency in three soils by the HYDRUS-1D and -2D simulations. Soil Till. Res. 194, 104342 https://doi.org/10.1016/j.still.2019.104342.

Zhao, Y., Li, Y., Wang, J., Pang, H., Li, Y., 2016. Buried straw layer plus plastic mulching reduces soil salinity and increases sunflower yield in saline soils. Soil Till. Res 155, 363–370. https://doi.org/10.1016/j.still.2015.08.019.